

## Title Page

CRB2 in immature photoreceptors determines the superior-inferior symmetry of the developing retina to maintain retinal structure and function

Peter M. Quinn<sup>1</sup>, Celso Henrique Alves<sup>1</sup>, Jan Klooster<sup>2</sup>, Jan Wijnholds<sup>1,2\*</sup>.

<sup>1</sup>Department of Ophthalmology, Leiden University Medical Center, 2300 RC, Leiden, The Netherlands.

<sup>2</sup>Netherlands Institute for Neuroscience, Royal Netherlands Academy of Arts and Sciences, 1105 BA, Amsterdam, The Netherlands.

\*To whom correspondence should be addressed-~~at~~:

~~Dr.~~ Jan Wijnholds.

Fax: +31715268270

Telephone: +31715269269

Email: J.Wijnholds@lumc.nl

## Abstract

The mammalian apical-basal determinant Crumbs homolog-1 (CRB1) plays a crucial role in retinal structure and function by the maintenance of adherens junctions between photoreceptors and Müller glial cells. Patients with mutations in the *CRB1* gene develop retinal dystrophies, including early-onset retinitis pigmentosa and Leber congenital amaurosis. Previously, we showed that *Crb1* knockout mice developed a slow-progressing retinal phenotype at foci in the inferior retina, while specific ablation of *Crb2* in immature photoreceptors lead to an early-onset phenotype throughout the retina. Here, we conditionally disrupted one or both alleles of *Crb2* in immature photoreceptors, on a genetic background lacking *Crb1*, and studied the retinal dystrophies thereof. Our data showed that disruption of one allele of *Crb2* in immature photoreceptors caused a substantial aggravation of the *Crb1* phenotype in the entire inferior retina. The photoreceptor layer showed early-onset progressive thinning limited to the inferior retina while the superior retina maintained intact. Surprisingly, disruption of both alleles of *Crb2* in immature photoreceptors further aggravated the phenotype. Throughout the retina, photoreceptor synapses were disrupted and photoreceptor nuclei intermingled with nuclei of the inner nuclear layer. In the superior retina, the ganglion cell layer appeared thicker due to ectopic nuclei of photoreceptors. In conclusion, the data suggests that that CRB2 is required to maintain retinal progenitor and photoreceptor cell adhesion at the adherence zone and prevent uncontrolled photoreceptor ingression into the immature inner retina. We hypothesize, from these animal models, that decreased levels of CRB2 in immature photoreceptors adjust retinitis pigmentosa due to loss of CRB1 into Leber congenital amaurosis -phenotype due to loss of CRB1.

## Introduction

In humans, the Crumbs homolog-1 (*CRBI*) gene is mutated in a diverse spectrum of retinal dystrophies with variable phenotypes, including autosomal recessive Leber congenital amaurosis (LCA) and retinitis pigmentosa (RP) (1–3). Despite a genetic overlap, these are two clinically distinct inherited retinal dystrophies (4). Variations in the *CRBI* gene account for 7% to 17% of LCA cases as well as and 3% to 9% of nonsyndromic ~~cases of~~ autosomal recessive ~~retinitis pigmentosa (RP) cases~~ (5, 6). Leber congenital amaurosis (~~LCA~~) is a group of early-onset retinal dystrophies leading to blindness from near birth typically characterised by abnormal pupillary reflex, nystagmus, and non-recordable or severely attenuated electroretinogram (ERG) responses (7–11). Mutations in the *CRBI* gene cause LCA type 8 which is characterised by a thickening and abnormal layering of the retina not observed in other types of LCA (2, 12, 13). However, some LCA causing *CRBI* mutations have been associated with an unchanged or thinner retina (14, 15). Retinitis pigmentosa is a clinically heterogeneous disorder characterised by night blindness and progressive loss of visual field due to degeneration of rod ~~than cone~~ photoreceptors (4). Mutations in the *CRBI* gene cause RP type 12 which is characterised by a preservation of the para-arteriolar RPE (PPRPE) and progressive loss of visual field in early childhood due to macular involvement (1, 16). However, disease onset in *CRBI*-RP is highly variable with some patients showing symptoms after the first decade of life (7). Other *CRBI* related clinical features include Coats-like exudative vasculopathy, pigmented paravenous chorioretinal atrophy, macular atrophy, nanophthalmos, keratoconus, and RP without PPRPE (14, 17–23). Despite more than 230 pathogenic variants being identified for the *CRBI* gene (see <http://exac.broadinstitute.org/transcript/ENST00000367400> and <http://databases.lovd.nl/shared/variants/CRB1>) there is not a clear genotype-phenotype correlation.

In mammals, there are three CRB protein family members, CRB1-3. CRB1 and CRB2 proteins have large extracellular domains comprised of epidermal growth factor-like and laminin-A globular domains, a single transmembrane domain, and a short intracellular domain of 37 amino acids containing a FERM protein binding motif adjacent to a C-terminal PDZ protein binding motif (24). CRB3 shares with CRB1 and CRB2 the short intracellular and single transmembrane domain, but

CRB3 lacks the large extracellular domain. The C-terminal amino-acids ERLI in the PDZ domain allow~~s~~ for interaction of the CRB proteins with specific PDZ-binding adaptor proteins, such as PALS1 and PAR6 (25, 26). Interaction with PALS1 leads to the assembly of a core CRB complex. PALS1 binds through its N-terminal L27 protein-binding domain to the L27 domain of multiple PDZ-domain proteins MUPP1 or PATJ (27). In the retina, the CRB complex contributes to the maintenance of adherens junctions between retinal progenitor cells, Müller glial cells, and rod and cone photoreceptors cells, being crucial for retinal structure and function. The CRB complex is located in the aforementioned cell types at the subapical region (SAR) adjacent to adherens junctions (AJs) at the outer limiting membrane (OLM) (28–30). The localisation of CRB1 and CRB2 at the subapical region is the same in Müller glial cells of mice and human (30–34). However, there are some differences of localisation of the CRB proteins in photoreceptors of mouse versus human. Mouse photoreceptors do not express the CRB1 protein, although *Crb1* transcripts are detectable in these cells (30, 32, 35). ~~In human,~~ ~~S~~studies performed using human post-mortem retina demonstrated that the CRB1 protein localis~~es~~es at the subapical region of photoreceptors, while CRB2 protein localis~~es~~es at a distance from the subapical region in the photoreceptor inner segments (31, 34). ~~SomeA-number of~~ rodent mutant *CRB* models with naturally-occurring or introduced mutations in the *Crb1* gene have been described (3, 28–31, 36–42). ~~However,~~~~But~~ these models cannot be used to test the efficacy of photoreceptor-specific gene therapy vectors expressing *CRB2* nor reveal all retinal physiological functions of CRB2 in immature photoreceptors.

Similar to mice lacking CRB1, retinal dystrophy models of other CRB complex members such as CRB2, PALS1 (also called MPP5) and MPP3 showed disruptions of adherence junctions at the OLM (28, 39, 43–45). Recent studies revealed ~~that~~ a mild or severe retinal phenotype in *Crb1* mice ~~is~~ dependent on the levels of CRB2 in retinal progenitor cells (29, 31). Mice lacking CRB1 show retinal dystrophy at foci in the inferior retina, with protrusion of rows of photoreceptor nuclei into the inner- and outer segment layer and displacement of photoreceptor nuclei into the photoreceptor synaptic layer. These mice lacking CRB1 mimic a slow progressing RP-like phenotype (30). Loss of mouse CRB2 specifically in retinal radial glial progenitor cells or immature photoreceptors leads to early

disruption of the retinal lamination throughout the retina with a severe attenuation of the retinal function. The phenotype of the retinas of these mice mimics an early-onset RP-like phenotype (28, 39). Loss of CRB1 and CRB2 in progenitor cells results in a thickening of the retina due to overgrowth of late-born retinal cell types such as photoreceptors, Müller glial cells and bipolar cells (29). Recent work on *CRB* gene therapy suggested the need for CRB proteins in adjacent Müller glial cells and photoreceptors to maintain a functional adult retina (3, 34).

Here, to investigate the physiological role(s) of CRB2 in photoreceptors and adjacent retinal progenitor and Müller glial cells we studied the conditional disruption of one or both alleles of CRB2 in immature photoreceptors on a genetic background lacking *Crb1*. Our data show that reduced levels of CRB2 in immature photoreceptors resulted in a phenotype similar to early-onset RP. While, full ablation of *Crb2* from immature photoreceptors produced a phenotype that mimics mimicking LCA. The severity of phenotype is significantly increased in retinas lacking CRB1 with reduced levels of CRB2 in immature photoreceptors compared to retinas only lacking CRB1. These double mutant retinas showed extensive lamination defects in the inferior retina, photoreceptor cell death and loss of retinal activity as measured by electroretinography (ERG). Interestingly, retinas with reduced levels of CRB2 in immature photoreceptors showed a most severe phenotype at the inferior side of the retina, whereas complete loss of CRB2 further aggravated the phenotype and showed a most severe phenotype at the superior side of the retina. The retinal dystrophy models showed, therefore, retinal superior/inferior asymmetry of retinal degeneration in the superior versus inferior retina, suggesting an important role for CRB2 in immature photoreceptors in determining the superior-inferior symmetry of the developing retina in order to maintain retinal structure and function.

## Results

### Reduced levels of CRB2 in immature photoreceptors leads to retinal function impairment

Previously, we studied the contribution of CRB2 in retinal progenitors to the CRB1 retinal phenotype, in these studies the *Crb2* gene was ablated in retinal progenitors and therefore also in photoreceptors

and Müller glial cells (29, 31). To study the contribution of CRB2 in immature photoreceptors to the CRB1 phenotype, we compared the phenotypes of retinas with lowered levels of CRB2 in immature photoreceptors, *Crb1<sup>KO</sup>Crb2<sup>Low-imPRC</sup>*, ~~with retinas~~ with loss of CRB2 in immature photoreceptors, *Crb1<sup>KO</sup>Crb2<sup>ΔimPRC</sup>*, and with littermate control mice knockout for CRB1 but with normal levels of CRB2. Schematic models on the presence of CRB1 and CRB2 in progenitor cells, Müller glial cells, rod and cone photoreceptors cells are shown in Supplementary Material, Fig. S1.

Both the *Crb1<sup>KO</sup>Crb2<sup>ΔimPRC</sup>* and *Crb1<sup>KO</sup>Crb2<sup>Low-imPRC</sup>* mice were fertile, but the *Crb1<sup>KO</sup>Crb2<sup>ΔimPRC</sup>* mice showed a reduced Mendelian ratio of progeny than expected when analysed at postnatal day (P) 10 (Supplementary Material, Fig. S2A). Previously we reported a high incidence of hydrocephalus in the that *Crb2<sup>ΔimPRC</sup>* (39) mice had a high incidence of hydrocephalus. Here when backcrossed onto 100% C57BL/6J01aHsd genetic background all *Crb1<sup>KO</sup>Crb2<sup>ΔimPRC</sup>* mice developed severe hydrocephalus. The cause of hydrocephalus is not clear but may be due to leakage of the Cre driver in non-specific areas such as the brain. Hydrocephalous has also been reported in *aPKC λ<sup>fllox/fllox</sup>/Crx-cre* mice (46). In *Yap*-deficient mice the apical integrity of ventral aqueduct is compromised, showing disruption of the CRB complex and adherens junctions, leading to hydrocephalus (47). This highlights a possible role for CRB proteins in the ependymal cells of the ventral aqueduct. However, it is unlikely to cause or affect the retinal phenotypes we observed. -These *Crb1<sup>KO</sup>Crb2<sup>ΔimPRC</sup>* mice showed severe loss of bodyweight from postnatal day 9 (P9; Supplementary Material, Fig. S2C) and died between the second and third postnatal weeks (Supplementary Material, Fig. S2B and D). Therefore the Retinal function by electroretinography could was not be assessed in *Crb1<sup>KO</sup>Crb2<sup>ΔimPRC</sup>* retina due to reaching a humane endpoint. ThereforeTherefore, we only analysed the retinal function of the *Crb1<sup>KO</sup>Crb2<sup>Low-imPRC</sup>* that which do not show signs of not have hydrocephalus.

Mice lacking CRB1 showed disruptions at the OLM but normal retinal function as measured by electroretinography (ERG) (30). Also, *Crb2<sup>Low-imPRC</sup>* mice with reduced levels of *Crb2* showed normal retinal function as measured by ERG but in this case without disruptions at the OLM (39). Here, we performed ERG in 1-, 3-, and 6-months-old *Crb1<sup>KO</sup>Crb2<sup>Low-imPRC</sup>* double mutant mice and ~~in~~ age-

matched control mice (Fig. 1). At 1-month of age, a reduction in scotopic a-wave but not b-wave amplitudes was detectable (Fig. 1A). Analysis of the b/a ratio showed a higher ratio in *Crb1<sup>KO</sup>Crb2<sup>Low-imPRC</sup>* mice than control mice (Fig. 1B). ~~Further loss of retinal function was detected~~ At 3- and 6-months of age there was further loss of retinal function. Both the scotopic a- and b-wave amplitudes showed significant reductions (Fig. 1C and D). The photopic b-wave amplitudes showed a significant reduction at 3-months of age but only at high stimulus intensity (Fig. 1E). The flicker electroretinogram showed reductions at 3- and 6-months of age in ranges A and B, the rod pathway and the cone ON-pathway, respectively (Fig. 1F). Together the electroretinography data showed that removal of one allele of CRB2 in immature photoreceptors leads to a decrease in photoreceptor function from 1-month of age, suggesting an early-onset and progressive deterioration of the rod and cone systems.

### **Reduced levels of CRB2 in immature photoreceptors results in a severe inferior retinal phenotype**

Morphological analysis of the superior and inferior retina of *Crb1<sup>KO</sup>Crb2<sup>Low-imPRC</sup>* mice was carried out from P10 till 6-months of age. The superior part of the control retina (Fig 2A, D, G) and the *Crb1<sup>KO</sup>Crb2<sup>Low-imPRC</sup>* retina (data not shown) was unaffected at 1-month of age. However, morphological alterations of the *Crb1<sup>KO</sup>Crb2<sup>Low-imPRC</sup>* superior retina were found adjacent to the optic nerve head (ONH) and extended to the inferior side of the retina from the ONH to the peripheral inferior retina (Supplementary Material, Fig. S3A). In 1-month old *Crb1<sup>KO</sup>Crb2<sup>Low-imPRC</sup>* retinas at the superior side close to the ONH (Fig. 2B) and at the inferior side (Fig. 2C ~~and Supplementary Material, Fig. S3B~~), we detected half-rosettes of the outer nuclear layer. ~~Additionally, we detected,~~ and focal protrusions of nuclei from the outer nuclear layer into the inner- and outer segment layer.

Interestingly, the half-rosettes had an organised OLM and photoreceptor segments (Fig. 2C). The OLM was ~~well~~-visible at the superior side in the entire control retina (Fig. 2D) and *Crb1<sup>KO</sup>Crb2<sup>Low-imPRC</sup>* retina (~~data not shown~~), on histological sections analysed at 1-, 3-, and 6-months of age (Overview stitches 1-, 3-, and 6-months of age, Supplementary Material, Fig. S2, Fig. S3 and Fig. S4).

Though close to the ONH of the *Crb1<sup>KO</sup>Crb2<sup>Low-imPRC</sup>* retina the OLM showed disruptions (Fig. 2B, E, and H). The *Crb1<sup>KO</sup>Crb2<sup>Low-imPRC</sup>* inferior retina showed frequent disruptions and loss of the OLM except for in the most-peripheral retina (Fig. 2C, F and I; Supplementary Material, Fig. S3A). The *Crb1<sup>KO</sup>Crb2<sup>Low-imPRC</sup>* inferior retina showed a progressive loss of photoreceptor cells at the degenerative foci at 3-months (Fig. 2F; [Supplementary Material, Fig. S4A](#)) and 6-months of age (Fig. 2I; [Supplementary Material, Fig. S4B](#)). At 3- and 6-months of age abnormalities in the choroid and retinal blood vasculature became detectable (Fig. 2F and I, respectively).

At 6-months of age, the *Crb1<sup>KO</sup>Crb2<sup>Low-imPRC</sup>* retinal pigment epithelium (RPE) layer and the inner retina including the ganglion cell layer (GCL) showed signs of degeneration (Fig. 2I). In the peripheral *Crb1<sup>KO</sup>Crb2<sup>Low-imPRC</sup>* inferior retina a sharp boundary between the area of phenotype and the area of the non-affected retina was observed at 1, 3 and 6-months of age (Supplementary Material, Fig. [S53B-DA-C](#)). The spread of the *Crb1<sup>KO</sup>Crb2<sup>Low-imPRC</sup>* inferior phenotype from the ONH to the peripheral inferior retina was variable between mice of the same age. The outer nuclear layer in the inferior *Crb1<sup>KO</sup>Crb2<sup>Low-imPRC</sup>* retinas was thickened at P10, P14, and 1-month of age and became thinned at 3-months of age, whereas the thickness of the outer nuclear layer of the superior retina did not significantly change from P10 till 3-months of age (Fig. 2J). [Total retinal thickness was decreased in the inferior versus superior \*Crb1<sup>KO</sup>Crb2<sup>Low-imPRC</sup>\* retina and control retina \(Fig. 2K\).](#)

To further study the disruptions at the OLM observed in the histological analysis, we analysed the localization of proteins at the subapical region (Fig. 3A-C: CRB2, D-F: PALS1, G-I: multiple-PDZ-protein MUPP1) and adherens junctions (Fig. 3A-C: p120-catenin, D-F: N-cadherin,) by immunohistochemistry on 3-months-old control and *Crb1<sup>KO</sup>Crb2<sup>Low-imPRC</sup>* retinas. In control retinas, we found subapical region markers adjacent to adherens junctions at the OLM (Fig. 3 A, D, G). In the superior *Crb1<sup>KO</sup>Crb2<sup>Low-imPRC</sup>* retina, the disruptions of the OLM were limited to the region immediately adjacent to the ONH, concomitant with the protrusion of photoreceptor nuclei into the inner- and outer segment layer. The disruptions at foci at the OLM were confirmed by staining with markers of the subapical region and adherens junctions (Fig. 3B, E, H). In the inferior retina, at foci of

degeneration the subapical region and adherens junctions were severely disrupted and showed at these foci loss of photoreceptors (Fig. 3C, F, I).

In control retina, SOX9-positive Müller glial cell nuclei reside in the inner nuclear layer (Fig. 4 A).

Ectopic SOX9-positive Müller glial cell nuclei in the outer nuclear layer further exemplified loss of conventional lamination in the three-month-old  $Crb1^{KO}Crb2^{Low-imPRC}$  retina.

Loss of regular lamination in the three-month-old  $Crb1^{KO}Crb2^{Low-imPRC}$  retina was further exemplified by ectopic SOX9-positive Müller glial cell nuclei in the outer nuclear layer (Fig. 4B, C, arrows). In the affected

areas, staining for glutamine synthetase appeared less regular especially apically at the OLM and in

the outer nuclear layer (Fig. 4B and C). The superior control retina showed localization of glial

fibrillary acidic protein (GFAP) at the endfeet of Müller glial cells (Fig. 4D).  $Crb1^{KO}Crb2^{Low-imPRC}$

retina showed moderate upregulation of intermediate filament GFAP expression in Müller glial cells

in the superior retina (Fig. 4E), this was even more pronounced in the inferior retina (Fig. 4F). In the

$Crb1^{KO}Crb2^{Low-imPRC}$  inferior retina, GFAP expression was detected in apical processes wrapping

around photoreceptors (Fig. 4F, arrow). Immunohistochemistry was performed to test whether the

loss of retinal lamination in  $Crb1^{KO}Crb2^{Low-imPRC}$  mice affected the retinal vasculature as well as

infiltration of microglial cells. We stained with markers for activated (CD11b) and resting state

(CD45) microglial cells and markers for endothelial cells and retinal vasculature such as Von

Willebrand Factor (vWF) and Griffonia simplicifolia B4-isolectin (IB4). Microglial phagocytosis of

living photoreceptors might contribute to retinal degeneration (48). In control retina, the microglial

cells, the endothelial cells, and vasculature were restricted to the inner retina (Fig. 4G and J).

Abnormalities of the vasculature system were not observed at the superior side of the  $Crb1^{KO}Crb2^{Low-imPRC}$  retina close to the ONH (Fig. 4H and K). However, but in the inferior retina abnormal

neovascularisation was detected (Fig. 4I and L). Ectopic localization of microglial cells was not

observed at the superior side of the  $Crb1^{KO}Crb2^{Low-imPRC}$  retina, but was detected close to the ONH

(Fig. 4H and K) and even stronger at the inferior side of the retina (Fig. 4I and L). The data suggested

ectopic hematopoietic and activated microglial cells in the degenerating  $Crb1^{KO}Crb2^{Low-imPRC}$

photoreceptor layer. Interestingly, at some locations, the microglial cells, the hematopoietic cells, and the endothelial cells were closely associated.

To test whether the severe disruption of the retinal lamination in 3-month-old *Crbl<sup>KO</sup>Crb2<sup>Low-imPRC</sup>* retina had affected the photoreceptor synapses and the localization and structure of photoreceptors we stained with several markers for photoreceptors. In the control retina (Fig. 5A), and the *Crbl<sup>KO</sup>Crb2<sup>Low-imPRC</sup>* superior retina including close to the ONH, the inner retina, and the outer retina appeared ~~healthy~~normal (Fig. 5B). Whereas at the inferior side of the *Crbl<sup>KO</sup>Crb2<sup>Low-imPRC</sup>* retina only a few photoreceptors ~~could be were~~ detected (Fig. 5C). In the *Crbl<sup>KO</sup>Crb2<sup>Low-imPRC</sup>* inferior retina, the inner retina was relatively unaffected except for gaps of nuclei at foci in the inner nuclear layer (Fig. 5C).

At the superior sides of control retina (Fig. 5D) and of the *Crbl<sup>KO</sup>Crb2<sup>Low-imPRC</sup>* retina (data not shown) the rod and cone photoreceptor nuclei and inner and outer segments were orderly organized. Some photoreceptors protruded into the outer plexiform layer in the *Crbl<sup>KO</sup>Crb2<sup>Low-imPRC</sup>* superior retina but only close to the ONH (Fig. 5E, boxed area). At the inferior side of the *Crbl<sup>KO</sup>Crb2<sup>Low-imPRC</sup>* retina only a few rod and cones photoreceptors survived (Fig. 5F). In the *Crbl<sup>KO</sup>Crb2<sup>Low-imPRC</sup>* superior retina near the ONH, we found sporadic internalisation of S-opsin which ~~usually~~is expressed in the inner and outer segments of photoreceptors (Fig. 5G and H, boxed area). In the *Crbl<sup>KO</sup>Crb2<sup>Low-imPRC</sup>* inferior retina, we found ~~the~~ loss of photoreceptor segments as marked by recoverin (Fig. 5C), internalised rhodopsin, ~~cone-arrestin (Fig. 5F, boxed area)~~, and S-opsin (Fig. 5I, boxed area).

The gaps in the inner nuclear layer presumably reside at areas where ectopic blood vessels pass through the inner nuclear layer (Fig. 5C and 4L). Further analysis indicated that other inner retinal cell types such as PKC $\alpha$ -positive bipolar cells and calretinin-positive amacrine cells were not ectopically localized in the superior *Crbl<sup>KO</sup>Crb2<sup>Low-imPRC</sup>* retina (Fig. 5A-B, 5J-K and data not shown). In the *Crbl<sup>KO</sup>Crb2<sup>Low-imPRC</sup>* inferior retina, nevertheless, bipolar cell dendrites were found protruding into the outer nuclear layer (Fig. 5L). MPP4 is ~~normally abundantly usually~~ expressed at the synapses of photoreceptors being in a complex with other synaptic proteins such as PSD-95 and TMEM16b (49,

50). In the control retina, photoreceptor synaptic proteins such as MPP4 localized at the outer plexiform layer (Fig. 5J). In the *Crb1<sup>KO</sup>Crb2<sup>Low-imPRC</sup>* superior retina, photoreceptor synaptic proteins localized correctly and were detectable only at the outer plexiform layer (Fig. 5K), whereas in the *Crb1<sup>KO</sup>Crb2<sup>Low-imPRC</sup>* inferior retina ectopic synapses were detected in the photoreceptor nuclear layer (Fig. 5L).

In summary, whereas we had previously shown that reduced levels of CRB2 in immature photoreceptors caused no retinal phenotype in the first ~~five~~ months (39), and that loss of CRB1 in progenitor and Müller glial cells caused a ~~very~~-mild inferior-lateral retinal phenotype (30, 37). Here, we suggest ~~that~~ moderately reduced levels of CRB2 in immature photoreceptors with concomitant loss of CRB1 in progenitor and Müller glial cells results in a severe early-onset RP phenotype at the inferior side of the retina.

### **Loss of CRB2 in immature photoreceptors results in a phenotype that is more severe in the superior than in the inferior retina**

Previously, we analysed retinas lacking CRB2 in immature rod and cone photoreceptors that developed an early RP phenotype due to loss of photoreceptors throughout the retina (28). The retinas showed retinal disorganization of the photoreceptor layer with an overall proper lamination of the inner retina. In other studies, we analysed retinas lacking CRB1 and CRB2 specifically in immature radial glial progenitor cells that developed an LCA phenotype with overgrowth of late-born retinal cell types mimicking in part the thickened retina observed in patients with LCA due to loss of CRB1 (29, 31). Here, we examined retinas lacking CRB1 with loss of CRB2 specifically in immature rod and cone photoreceptor cells and show ~~that~~ these develop a novel LCA phenotype with thickened retina, without retinal overgrowth but with retinal redistribution of photoreceptors. No morphological defects were detected during ~~very~~-early retinal development at embryonic day 13.5 (E13.5). ~~N~~, but ~~nevertheless~~ disruptions at the OLM were detected from ~~embryonic day EE~~15.5 in the *Crb1<sup>KO</sup>Crb2<sup>ΔimPRC</sup>* mice as previously detected in *Crb2<sup>ΔimPRC</sup>* mice (39) (data not shown). From E17.5

onwards ectopic *Crb1<sup>KO</sup>Crb2<sup>ΔimPRC</sup>* photoreceptor nuclei were detected in the GCL, half rosettes were found apically in the nuclear blast layer, and the lamination of the retina was significantly disturbed (Fig. 6B and C). Surprisingly, at E17.5 and P1, the *Crb1<sup>KO</sup>Crb2<sup>ΔimPRC</sup>* superior retina shows a more severe phenotype with complete lack of OLM, whereas in the inferior retina there were still regions with an apparent intact OLM (Fig. 6B-C and E-F). Transmission electron microscopic analyses at E17.5 showed electron dense adherens junctions in the control retina (Fig. 6J) but ~~the~~ loss of adherens junctions in the *Crb1<sup>KO</sup>Crb2<sup>ΔimPRC</sup>* retinas, as well as lack of inner segments and the appearance of ectopic nuclei close to the retinal pigment epithelium (Fig. 6K). At P1 and P5 a distinct inner plexiform layer and a GCL were formed in the *Crb1<sup>KO</sup>Crb2<sup>ΔimPRC</sup>* retina, ~~However, but~~ at the superior retina as well as at the inferior retina close to the ONH many ectopic ~~additional~~ nuclei resided in the GCL whereas less ectopic cells accumulated at the inferior side (Fig. 6E-F, H-I, and L-M). In the control retina the outer nuclear layer, ~~the~~ outer plexiform layer (OPL), and ~~the~~ inner nuclear layer formed at P5 (Fig. 6G). ~~HoweverWhile,But~~ in the *Crb1<sup>KO</sup>Crb2<sup>ΔimPRC</sup>* retina, these layers fused to a single broad neuroblast layer (NBL) (Fig. 6H and I).

Since the earliest observed effects were detected at the OLM, we analysed the subapical region for disruptions using subapical markers CRB2, PAR3, PALS1, and MUPP1 and loss of adherens junction markers p120-catenin, β-catenin, and N-cadherin. As expected from the above morphological analysis (Fig. 6E), the subapical region and adherens junctions were ~~lost entirely completely lost~~ in the *Crb1<sup>KO</sup>Crb2<sup>ΔimPRC</sup>* superior retina (Fig. 7B, E, H, K) and the inferior retina close to the ONH (data not shown). In the morphologically less affected inferior retina (Fig. 6F), the subapical region and adherens junctions were detectable but showed disruptions at foci where nuclei protruded into the inner- and outer segment layer (Fig. 7C, F, I, L).

### **Loss of CRB2 in immature photoreceptors affects mitosis and apoptosis**

Previously we ablated either CRB2 or both CRB1 and CRB2 specifically in early retinal progenitors and their derived cells. In ~~these-those~~ retinas, we detected an increase in progenitor cells as well as late-born retinal cell types such as rod photoreceptors, bipolar cells, and Müller glial cells, and detected an increase in programmed cell death in the developing retina (28, 29). The Crx-Cre

transgenic mice used in the current study expressed Cre recombinase from ~~embryonic day 12.5~~ (E12.5) in immature postmitotic photoreceptors (46, 51). In the *Crb1<sup>KO</sup>Crb2<sup>ΔimPRC</sup>* retina, the Cre recombinase therefore ablated CRB2 in immature post-mitotic rod and cone photoreceptors but not in the retinal radial glial progenitor cells, whereas CRB1 was lost from radial glial progenitor cells including all derived cells such as Müller glial cells that would ~~typic~~ normally express CRB1 (Supplementary Material, Fig. S1).

To check whether loss of CRB2 protein in immature post-mitotic photoreceptors ~~affected had an effect on~~ the adjacent early retinal progenitors we stained for mitotic markers. Anti-phospho-histone ~~-~~H3 (anti-pH3) stains M-phase nuclei that ~~normally~~ reside most apically in the retina (Fig. 8A). Ectopic anti-pH3 positive nuclei were detected in the *Crb1<sup>KO</sup>Crb2<sup>ΔimPRC</sup>* inner retina and the GCL at E17.5 and P1 (Fig. 8B, C, and Fig. 8G). A significant increase in the total number of anti-pH3 positive nuclei was seen in *Crb1<sup>KO</sup>Crb2<sup>ΔimPRC</sup>* retina when compared to *Crb1<sup>KO</sup>Crb2<sup>Low-imPRC</sup>* and control retina at P1 (Fig. 8G) but not at E17.5 (data not shown). Ki67 is a marker for cycling cells ~~and is being~~ expressed ~~during their~~ G2, M, and ~~the~~ latter half of the S phase. In ~~the~~ control developing retina, the newly formed GCL contained differentiated ganglion cells and displaced Starburst amacrine cells but no cycling cells (Fig. 8A, G, and data not shown). In the *Crb1<sup>KO</sup>Crb2<sup>ΔimPRC</sup>* retina, ectopic anti-Ki67 positive cells were detected in the GCL at E17.5 and P1 (Fig. 8B, C, and Fig. 8H). Next, we checked whether or not there was an increase in the pool of progenitor cells, ~~but~~ the total number of anti-Ki67 positive cells was not different from ~~that of the~~ *Crb1<sup>KO</sup>Crb2<sup>Low-imPRC</sup>* or control retina at P1 (Fig. 8H). We detected, however, an increase in the number of apoptotic cells at both E17.5 and P1 in *Crb1<sup>KO</sup>Crb2<sup>ΔimPRC</sup>* retina (Fig. 8I and Supplementary ~~M~~aterial, Fig. S4). In summary, loss of CRB1 from retinal progenitor cells with specific loss of CRB2 in immature photoreceptors resulted in an increased number of progenitors in M-phase concomitant with an increase in retinal cells undergoing programmed cell death.

### **Aberrant localization of photoreceptor cells in the inner retina and ganglion cell layer of *Crb1<sup>KO</sup>Crb2<sup>ΔimPRC</sup>* retina**

To explore if the ectopic cycling cells in the inner retina had any effects on the localization of early-born post-mitotic photoreceptors cells, we stained post-mitotic photoreceptors with anti-recoverin. These cells were typically found most apically in P1 retina (Fig. 8D). We found an increased number of ectopic recoverin-positive cells in *Crb1<sup>KO</sup>Crb2<sup>ΔimPRC</sup>* retina when compared to *Crb1<sup>KO</sup>Crb2<sup>Low-imPRC</sup>* and control retina at P1. These cells were mislocalised at P1 in the bottom part of the neuroblast layer and in the GCL (Fig. 8E and F).

The early developing *Crb1<sup>KO</sup>Crb2<sup>ΔimPRC</sup>* retina showed differences in superior/inferior asymmetry in retinal dystrophy. Therefore, we examined the P14 retina for thickness and localization of photoreceptor cells. Previously we did so for retinas lacking CRB1 and CRB2 in progenitor cells and found the ectopic localization of photoreceptors and inner retinal cells in the GCL. At P14 the outer nuclear layer and inner nuclear layer in the *Crb1<sup>KO</sup>Crb2<sup>ΔimPRC</sup>* retina were fused to a single nuclear layer (NL) of differentiated cells and lacked an outer plexiform layer, whereas this phenomenon was not detected in control or *Crb1<sup>KO</sup>Crb2<sup>Low-imPRC</sup>* retinas (Fig. 9A-C). Apically located rosettes of retinal cells were detectable in the most affected inferior part of the *Crb1<sup>KO</sup>Crb2<sup>Low-imPRC</sup>* retinas with low levels of CRB2, as well as in the superior and inferior parts of the *Crb1<sup>KO</sup>Crb2<sup>ΔimPRC</sup>* retinas with loss of CRB2 (Fig. 9B', C'). The GCL thickness was substantially increased in the inferior retina 0.75 mm from the ONH and in the entire superior retina in the *Crb1<sup>KO</sup>Crb2<sup>ΔimPRC</sup>*. The GCL thickness was not changed in the inferior-peripheral retina of *Crb1<sup>KO</sup>Crb2<sup>ΔimPRC</sup>* or in the *Crb1<sup>KO</sup>Crb2<sup>Low-imPRC</sup>* or control retina (Fig. 9A-C, C' and D). The increase in thickness in the GCL in the inferior side of *Crb1<sup>KO</sup>Crb2<sup>ΔimPRC</sup>* retina was limited to the first 0.75 mm from the ONH whereas the most peripheral retina showed the normal thickness of the GCL (Fig. 9D, C<sub>2</sub> and C''). The increase in thickness in the GCL at the superior side of the *Crb1<sup>KO</sup>Crb2<sup>ΔimPRC</sup>* retina was limited to the first 1.5 mm from the ONH but being thicker closest to the ONH and then thinning towards the peripheral retina (Fig. 9D).

Staining for recoverin showed an increase in misplaced cells into the basal part of the nuclear layer (bNL) and GCL of P14 *Crb1<sup>KO</sup>Crb2<sup>ΔimPRC</sup>* retina when compared to *Crb1<sup>KO</sup>Crb2<sup>Low-imPRC</sup>* or control retina (Fig. 9E). There was however not an increase in the total number of recoverin-positive cells. An increase in the number of ectopic recoverin-positive cells was found in the superior compared to the

inferior *Crb1<sup>KO</sup>Crb2<sup>ΔimPRC</sup>* retina (Fig. 9F). The ectopic photoreceptors were found to be mostly recoverin/rhodopsin double-positive rods, but mislocalised cones were also detected (Supplementary [Material](#), Fig. S5). However photoreceptor synaptic marker MPP4 could not be detected in the *Crb1<sup>KO</sup>Crb2<sup>Low-imPRC</sup>* retina at P14 (data not shown). Retinal neovascularization, as marked by IB4, was detected in the superior and inferior *Crb1<sup>KO</sup>Crb2<sup>ΔimPRC</sup>* fused outer and inner nuclear layer, as well as in the outer nuclear layer in *Crb1<sup>KO</sup>Crb2<sup>Low-imPRC</sup>* mouse retina (Supplementary [Material](#), Fig. S6).

## Discussion

In this study, we showed that (i) CRB2 levels in immature photoreceptors play a modulating role in determining the severities of CRB1 retinal dystrophies in mice; (ii) CRB2 plays [essentialimportant](#) roles in immature photoreceptors; (iii) loss of CRB2 localization at the subapical region adjacent to adherens junctions in immature photoreceptors disrupts the adhesion of immature retinal cell types at the OLM; (iv) CRB2 in immature photoreceptors determines the superior-inferior symmetry of the developing retina to maintain retinal structure and function; (v) physiological levels of CRB proteins in adjacent photoreceptors and Müller glial cells are [essentialimportant](#) for amelioration of CRB retinal dystrophies.

We showed here that [levels of CRB2 in immature photoreceptors modulated CRB1 retinal dystrophies in mice](#)~~CRB1 retinal dystrophies in mice were modulated by levels of CRB2 in immature photoreceptors~~. The data suggest ~~that the~~ CRB2 levels remaining in progenitor cells and derived Müller glial cells were insufficient to maintain a laminated retinal structure in *Crb1<sup>KO</sup>Crb2<sup>ΔimPRC</sup>* mouse retinas. Retinas lacking CRB1 and CRB2 in immature photoreceptors developed an LCA-like phenotype. We hypothesize ~~that~~ patients with mutations in the *CRB1* gene with lowered levels or reduced function of CRB2 in immature photoreceptors will display a more severe phenotype than the ones with normal levels of CRB2 in photoreceptors. Recently, we showed ~~that~~ CRB2 is present in fetal human radial glial progenitor cells in ~~the first~~ trimester retina, whereas CRB1 gets expressed

from the second trimester coinciding with the birth of photoreceptors and Müller glial cells ((52); unpublished data PQ and JW). The observed thickened retina, due to an increase in GCL thickness, in our *Crb1<sup>KO</sup>Crb2<sup>ΔimPRC</sup>* mice might, ~~therefore, therefore~~ mimic the thickened retina as found in LCA patients with mutations in the *CRB1* gene (12, 13).

The retinal phenotype was attenuated from LCA to early-onset RP in the *Crb1<sup>KO</sup>Crb2<sup>Low-imPRC</sup>* mouse retinas with half the reduced levels of CRB2 in immature photoreceptors and full levels of CRB2 in progenitors and derived Müller glial cells. We propose ~~that the~~ maintenance of physiological levels of CRB proteins in adjacent photoreceptors and Müller glial cells are necessary important for the amelioration of CRB retinal dystrophies.

In previous studies (39) we analysed retinas lacking CRB2 in immature retinas, *Crb2<sup>ΔimPRC</sup>* retinas. Here we detected a much more aggravated retinal phenotype in *Crb1<sup>KO</sup>Crb2<sup>ΔimPRC</sup>* mice. The *Crb2<sup>ΔimPRC</sup>* retinas showed a phenotype throughout the entire retina without fusion of the outer and inner nuclear layers mimicking early-onset RP, whereas the *Crb1<sup>KO</sup>Crb2<sup>ΔimPRC</sup>* retinas showed a phenotype in which the outer and inner nuclear layers fused throughout the entire retina mimicking LCA. Furthermore, in *Crb2<sup>ΔimPRC</sup>* retinas, we previously found sporadic abnormal localizations of photoreceptors in the GCL whereas in the *Crb1<sup>KO</sup>Crb2<sup>ΔimPRC</sup>* retinas we found extensive mislocalisation of photoreceptors in the GCL.

We hypothesize that CRB2 plays a critical important direct roles in maintaining adhesion between immature photoreceptors and progenitor cells besides a previously revealed role in E13.5 – P5 retinal progenitors (29). In previous studies, we analysed retinas with loss of CRB2 as well as CRB1 in radial glial progenitors, which showed in part a very similar retinal phenotype of LCA to the current studies on mice with loss of CRB2 in immature photoreceptors with concomitant loss of CRB1 from progenitor cells. Ablation of CRB2 or both CRB1 and CRB2 in cycling progenitors resulted in an increased number of progenitors with an increase in the number of late-born but not early-born retinal cell types ~~such as rod photoreceptors, bipolar cells and Müller glial cells but not of e.g. cone photoreceptors, horizontal, ganglion cells or early born amacrine cells~~ (28, 29). Our current data

described an increase in the number of phospho-Histone H3 positive mitotic cells but no increase in the total progenitor pool at P1 in *Crb1<sup>KO</sup>Crb2<sup>ΔimPRC</sup>* retinas compared to *Crb1<sup>KO</sup>Crb2<sup>Low-imPRC</sup>* retinas and *Crb1Crb2<sup>f/f</sup>* control retinas. The increase in pH3-positive cells suggests ~~that a~~ loss of CRB2 in immature photoreceptor cells caused an increased number of retinal progenitors in the M-phase of the cell cycle. The increased number of progenitors in M-phase did not result in a retina with an increased number of retinal cell types such as photoreceptors due to a concomitant increased programmed cell death throughout the P1 retina. The similar early onset of disruptions at the OLM in *Crb1<sup>KO</sup>Crb2<sup>ΔimPRC</sup>* retinas compared to retinas lacking CRB2 and CRB1 in progenitors suggest a significantmajor role for CRB2 in maintaining cellular adhesion in immature rod photoreceptors.

The early disruption of adhesion between immature retinal cell types at the OLM due to loss of CRB2 in immature photoreceptors allows a testable working hypothesis on the pathologic steps towards LCA. The adherence junctions at the OLM with interactions of rod and cone photoreceptors with radial glial progenitor cells become disrupted, resulting in displaced rows of photoreceptors and ectopic half-rosettes. The ectopic half-rosettes contain immature photoreceptors as well as cycling progenitors produced at its regular location at the OLM. The ectopic cycling progenitors produced new immature photoreceptors in the nuclear blast layer, ~~and/or in~~ the GCL, or both. The displaced photoreceptors in the nuclear blast layer either stay there or migrate along radial glial progenitor cells or immature Müller glial cells towards the GCL. Alternatively, ~~Or~~ the ectopic photoreceptors are born in the GCL.

Previously, Jacobson *et al.* using optical coherence tomography, found that *CRB1* patient LCA retinas had 1.5 times thicker retina than normal and ~~that~~ did not have the prototypic retinal layering.

Interestingly, they identified a single combined nuclear layer and a broad inner retinal zone, which they hypothesised, would be a layer with increased ganglion cells among synaptic and glial elements (53). Moreover, a *CRB1* patient with Familial Foveal Retinoschisis, a rare autosomal recessive disorder typified by cart-wheel lesion restricted to the macula, was described having a thickened IPL-GCL, due to schitic changes of the retinal layers (18). We instead hypothesise that this broad inner retinal layer found in postnatal human *CRB1* LCA patients is similar to the thickened retina in

*Crb1<sup>KO</sup>Crb2<sup>ΔimPRC</sup>* mice. Thus being broader ~~is due to the displacement or the ectopic birth of~~  
photoreceptors in the inner retina.

Previously we have shown that in the adult ~~wild-wild~~-type retina CRB2 is expressed at higher levels in the inferior ~~retina~~ ~~(inferiorly)~~ than in the superior retina ~~(superiorly)~~, and CRB1 is expressed at higher levels in the superior retina than the inferiorly retina (31). ~~This So, the CRB2 and CRB1 are expressed in~~indicates Highlighting, opposing gradients of CRB1 and CRB2 expression. The CRB1 protein is expressed in the adult retina only in Müller glial cells (32). The CRB2 is expressed in the adult retina in both Müller glial cells and photoreceptors (32). The gradient of high levels of CRB2 at the OLM at the inferior side of the adult ~~wild-wild~~-type retina compared to the relatively low levels at the superior side does not inform about the relative levels of CRB2 at the subapical region in Müller glial cells or photoreceptors. In the comparison of *Crb1<sup>KO</sup>Crb2<sup>Low-imPRC</sup>* retinas ~~compared to~~ *Crb1<sup>KO</sup>Crb2<sup>FF</sup>* control retinas, we reduced levels of CRB2 in all immature photoreceptors and detected the spread of the a very severe phenotype is spreading from the superior side of the ONH to the peripheral inferior retina at the inferior side and no phenotype at the superior side. From these data we hypothesisize that the levels of CRB2 at the inferior side are at lower and more critical levels in immature photoreceptors than at the superior side of the retina, therefore causing severe retinal degeneration at the inferior side of the *Crb1<sup>KO</sup>Crb2<sup>Low-imPRC</sup>* retinas. We early hypothesised suggested how variation of CRB2 levels in patients with mutations in the CRB1 gene mightay affect the severity of the disease. Similarly, based on clinical reports, we may-hypothesise that variation of CRB2 levels affects spread of disease in CRB1 patients. With some cases of LCA just affecting the inferior retina whiles other showing degeneration of all quadrants (14, 22, 53, 54).

In the comparison of *Crb1<sup>KO</sup>Crb2<sup>ΔimPRC</sup>* retinas compared to *Crb1<sup>KO</sup>Crb2<sup>Low-imPRC</sup>* retinas we further reduced levels of CRB2 to null in immature photoreceptors and detected a more severe phenotype at the superior side than at the inferior side. The latter data suggest that upon complete loss of CRB2 in immature photoreceptors the remaining levels of CRB2 in the progenitors and Müller glial cells are not sufficient to maintain adhesion at the OLM between the various retinal cell types. We hypothesisize therefore that CRB2 in immature photoreceptors determines the superior-inferior

symmetry of the developing retina to maintain retinal structure and function. We have previously suggested that CRB2 is a modifier of the CRB1 retinal phenotype in mice and the modifier function of CRB2 also became apparent in the current study (31).

## Materials and Methods

### Animals

Procedures concerning animals were performed with permission of the animal experimentation committee (DEC) of the Royal Netherlands Academy of Arts and Sciences (KNAW) and the ethical committee of the Leiden University Medical Center under permit number NIN 12.105. All mice used were maintained on a 100% C57BL/6JOLAHsd genetic background with a 12 h day-night cycle and supplied with food and water *ad libitum*. We crossed *Crbl<sup>-/-</sup>* mice (30) with *Crb2<sup>F/F</sup>CrxCre<sup>Tg/wt</sup> (Crb2<sup>ΔimPRC</sup>)* (39) mice to obtain *Crbl<sup>-/-</sup>Crb2<sup>F/F</sup>CrxCre<sup>Tg/wt</sup>* (*Crbl<sup>KO</sup>Crb2<sup>ΔimPRC</sup>*) and *Crbl<sup>-/-</sup>Crb2<sup>F/+</sup>CrxCre<sup>Tg/wt</sup> (Crbl<sup>KO</sup>Crb2<sup>Low-imPRC</sup>)* and Control *Crbl<sup>-/-</sup>Crb2<sup>F/+</sup>* and *Crbl<sup>-/-</sup>Crb2<sup>F/F</sup>* mice not expressing Cre. Subsequently, *Crbl<sup>KO</sup>Crb2<sup>Low-imPRC</sup>* and *Crbl<sup>-/-</sup>Crb2<sup>F/F</sup>* mice were crossed to generate *Crbl<sup>KO</sup>Crb2<sup>Low-imPRC</sup>*, *Crbl<sup>KO</sup>Crb2<sup>ΔimPRC</sup>*, and littermate Control mice. Analysis of *Crbl<sup>KO</sup>Crb2<sup>ΔimPRC</sup>* and *Crbl<sup>KO</sup>Crb2<sup>Low-imPRC</sup>* mice were performed using only male animals. Chromosomal DNA isolation and genotyping were performed as described previously (28, 39).

### Electroretinography (ERG)

Dark and light-adapted ERGs were performed under dim red light using an Espion E2 (Diagnosys, LLC, MA). ERGs were performed on 1-month-old (1M), 3M, and 6M *Crbl<sup>KO</sup>Crb2<sup>Low-imPRC</sup>* mice. Mice were anesthetized using 100 mg/kg ketamine and 10 mg/kg xylazine intraperitoneally, and the pupils were dilated using atropine drops (5 mg/mL). Mice were placed on a temperature regulated heating pad, and reference and ground electrodes were placed subcutaneously in the scalp and the base of the tail respectively. ERGs were recorded

from both eyes using gold wire electrodes. Hypromellose eye drops (3 mg/ml, Teva) were given between recordings to prevent eyes from drying. Single (Scotopic and Photopic ERG) or brief train (Flicker ERG) white (6500k)-flashes were used. Band-pass filter frequencies were 0.3 and 300 Hz. Scotopic recordings were obtained from dark-adapted animals at the following light intensities: -4, -3, -2, -1, 0, 1, 1.5, 1.9 log cd s/m<sup>2</sup> (55). Flicker recordings were obtained under a fixed light intensity of 0.5 log cd s/m<sup>2</sup> with varying frequency (0.5, 1, 2, 3, 5, 7, 10, 12, 15, 18, 20 and 30 Hz) (56, 57). Photopic recordings were performed following 10 minutes light adaptation on a background light intensity of 30 cd m<sup>2</sup> and the light intensity series used was: -2, -1, 0, 1, 1.5, 1.9 log cd s/m<sup>2</sup> (55).

### **Morphological analysis**

Eyes were collected at a range of time points from embryonic day E13.5 to 6M (n = 3-6/ age/ group). For morphological analysis, eyes were enucleated and fixed at room temperature with 4% paraformaldehyde in PBS for 20 minutes. After fixation, the eyes were dehydrated in 30, 50, 70, 90 and 100% ethanol for 30 minutes each. Eyes were orientated and embedded in Technovit 7100 (Kulzer, Wehrheim, Germany), according to the manufacturer's instructions and sectioned (3 μm). Slides were dried, counterstained with 0.5% toluidine blue and mounted under coverslips using Entellan (Merk, Darmstadt, Germany). Spidergrams of GCL thickness were measured every 250 μm from the optic nerve head (ONH) in P14 control, *Crb1*<sup>KO</sup>*Crb2*<sup>Low-imPRC</sup> and *Crb1*<sup>KO</sup>*Crb2*<sup>ΔimPRC</sup> mice (3 retinae per group (3 sections per retina)). ONL thickness was measured at 1mm from the ONH in P10, P14, 1M, and 3M *Crb1*<sup>KO</sup>*Crb2*<sup>Low-imPRC</sup> retinas superiorly and inferiorly (3-4 retina per time point (3 sections per retina)). All bright field images were taken on Leitz DRMB microscope (Leica Microsystems).

### **Immunohistochemical analysis**

For immunohistochemical analysis, eyes were incubated for 30 minutes in 4% paraformaldehyde in PBS for fixation and ~~in~~ 5% and then 30% sucrose in PBS for cryo-protection. Finally, retinae were orientated, embedded in Tissue-Tek O.C.T Compound (Sakura, Finetek), frozen and stored

at -20°C. Sections of 10 µm were made with a Leica CM1900 cryostat (Leica Microsystems). Sections for immunohistochemistry were blocked for 1 hour in 10% normal goat serum, 0.4% Triton X-100 and 1% bovine serum albumin (BSA) in PBS, incubated in a moist-chamber overnight at 4°C primary antibodies were diluted in 0.3% normal goat serum, 0.4% Triton X-100 and 1% BSA in PBS. After rinsing in PBS, the sections were incubated for 1 hour with complementary conjugated secondary antibodies and rinsed in PBS again. For quantification of dividing, cycling, and apoptotic cells retinal sections were stained with pH3 (E17.5 and P1), Ki67 (P1), and cleaved Caspase-3 (cCasp3) (E17.5 and P1) antibodies respectively. Total numbers of cells were determined by manually counting antibody-positive cells per area on digital images (3-5 retinae per time point (3-6 sections per retina)). P1 and P14 retinal sections were stained for quantification of photoreceptors (3-4 retinae per time point (3-6 sections per retina)).

### **Antibodies**

The following primary antibodies were used: Sox9 (1:250; Millipore), glutamine synthetase (1:250; BD Biosciences), CD45 (1:100; eBioscience), vWF (1:100; Dako), CD11b (1:100; ; eBioscience), IB4 (1:100; Sigma), Tuj1 (1:200; Biolegend), Recoverin (1:500; Millipore), Rhodopsin (1:500; Millipore), Cone Arrestin (1:500; Millipore), S-opsin (1:250; Millipore), PNA (1:200; Vector Lab), PKC $\alpha$  (1:250; BD Biosciences), Ki67 (1:100; BD Biosciences), pH3 (1:100; Millipore), cCasp3 (1:250; Cell signalling), MPP4 AK4 (1:300; homemade) (30), MPP5/PALS1 SN47 (1:200; homemade), CRB1 AK2 (1:200; homemade) (30), CRB2 EP13 (1:200; homemade), MUPP1 (1:200; BD Biosciences),  $\beta$ -catenin (1:250; BD Biosciences), p120-catenin (1:250; BD Biosciences), GFAP (1:200; Dako), N-cadherin (1:250; BD Biosciences). Fluorescent- labeled secondary antibodies were rabbit anti-chicken, goat anti- mouse, goat anti-rabbit or goat anti-rat IgGs conjugated to Cy3 (1:500; Jackson Immunoresearch, Stanford, USA and Invitrogen), Alexa 488 or Alexa 555 (Abcam) or Dylight549. Sections were mounted in Vectashield HardSet DAPI mounting media (Vector Laboratories). A Leica DM6B fluorescence microscope and Leica TCS SP8 confocal microscope

were used for Image acquisition. Image Analysis and processing were carried out using ImageJ and Adobe Photoshop CC2014.

### **Electron Microscopy**

Standard electron microscopy (EM) was performed as previously described (58). Eyes were fixed in 4% paraformaldehyde and 2% glutaraldehyde in PB for 24 hours. They were rinsed in 0.1-M sodium cacodylate buffered at pH 7.4 and postfixed for 2 hours in 1% OsO<sub>4</sub> in 0.1-M sodium cacodylate buffer (pH 7.4), containing 1.5% potassium ferricyanide. Eyes were embedded in epoxy resin and sections were cut, counterstained with uranyl acetate and lead citrate and examined in an FEI Tecnai electron microscope.

### **Statistical analysis**

All statistical analyses were performed using GraphPad Prism version 7 (GraphPad Software).

Normality of the distribution was tested by Kolmogorov–Smirnov test. Statistical significance was calculated by using *t*-test of 3–5 independent retinas/genotype/age. All values are expressed as mean ± SEM. Statistically significant values: \**P* < 0.05; \*\**P* < 0.01, \*\*\**P* < 0.001.

### **Acknowledgements**

The Authors thank Moira Goeman, Rawien Ramdien, [Nynke van de Haar](#), and Eline Nagel for technical assistance, Harald M. Mikkers and Monika Białocka for antibodies and all members of the Wijnholds Lab for advice on the manuscript.

### **Conflict of Interest statement**

None declared. The LUMC is the holder of patent application PCT/NL2014/050549, which describes the potential clinical use of CRB2; JW is listed as [the](#) inventor on this patent, and JW is an employee of the LUMC.

## Funding

This work was supported by the Foundation Fighting Blindness: TA-GT-0313-0607-NIN, TA-GT-0715-0665-LUMC, The Netherlands Organisation for Health Research and Development: ZonMw grant 43200004, Curing Retinal Blindness Foundation, Stichting Retina Nederland Fonds, Landelijke St. Blinden en Slechtienden, Rotterdamse Stichting, Blindenbelangen, St. Blindenhulp, St. Blinden-Penning, Algemene Nederlandse Vereniging ter Voorkoming van Blindheid (ANVVB), Gelderse Blinden Stichting and MaculaFonds.

## References

1. den Hollander,A.I., ten Brink,J.B., de Kok,Y.J., van Soest,S., van den Born,L.I., van Driel,M. a, van de Pol,D.J., Payne, a M., Bhattacharya,S.S., Kellner,U., *et al.* (1999) Mutations in a human homologue of *Drosophila crumbs* cause retinitis pigmentosa (RP12). *Nat. Genet.*, **23**, 217–21.
2. Richard,M., Roepman,R., Aartsen,W.M., van Rossum,A.G.S.H., den Hollander,A.I., Knust,E., Wijnholds,J. and Cremers,F.P.M. (2006) Towards understanding CRUMBS function in retinal dystrophies. *Hum. Mol. Genet.*, **15**, 235–243.
3. Quinn,P.M., Pellissier,L.P. and Wijnholds,J. (2017) The CRB1 complex: Following the trail of Crumbs to a feasible gene therapy strategy. *Front. Neurosci.*, **11**, 175.
4. Verbakel,S.K., van Huet,R.A.C., Boon,C.J.F., den Hollander,A.I., Collin,R.W.J., Klaver,C.C.W., Hoyng,C.B., Roepman,R. and Klevering,B.J. (2018) Non-syndromic retinitis pigmentosa. *Prog. Retin. Eye Res.*, 10.1016/j.preteyeres.2018.03.005.
5. Corton,M., Tatu,S.D., Avila-Fernandez,A., Vallespin,E., Tapias,I., Cantalapiedra,D., Blanco-Kelly,F., Riveiro-Alvarez,R., Bernal,S., Garcia-Sandoval,B., *et al.* (2013) High frequency of CRB1 mutations as cause of Early-Onset Retinal Dystrophies in the Spanish population. *Orphanet J. Rare Dis.*, **8**, 20.

6. Vallespin,E., Cantalapiedra,D., Riveiro-Alvarez,R., Wilke,R., Aguirre-Lamban,J., Avila-Fernandez,A., Lopez-Martinez,M.A., Gimenez,A., Trujillo-Tiebas,M.J., Ramos,C., *et al.* (2007) Mutation screening of 299 Spanish families with retinal dystrophies by Leber congenital amaurosis genotyping microarray. *Invest. Ophthalmol. Vis. Sci.*, **48**, 5653–61.
7. Talib,M., van Schooneveld,M.J., van Genderen,M.M., Wijnholds,J., Florijn,R.J., Ten Brink,J.B., Schalijs-Delfos,N.E., Dagnelie,G., Cremers,F.P.M., Wolterbeek,R., *et al.* (2017) Genotypic and Phenotypic Characteristics of CRB1-Associated Retinal Dystrophies: A Long-Term Follow-up Study. *Ophthalmology*, **124**, 884–895.
8. den Hollander,A.I., Roepman,R., Koenekoop,R.K. and Cremers,F.P.M. (2008) Leber congenital amaurosis: Genes, proteins and disease mechanisms. *Prog. Retin. Eye Res.*, **27**, 391–419.
9. Hasan,S.M., Azmeh,A., Mostafa,O. and Megarbane,A. (2016) Coat’s like vasculopathy in leber congenital amaurosis secondary to homozygous mutations in CRB1: a case report and discussion of the management options. *BMC Res. Notes*, **9**, 91.
10. Leber,T. (1869) Ueber Retinitis pigmentosa und angeborene Amaurose. *Albr. Von Graefes Arch Klin Exp Ophthalmol*, **15**, 1–25.
11. FRANCESCHETTI,A. and DIETERLE,P. (1954) [Diagnostic and prognostic importance of the electroretinogram in tapetoretinal degeneration with reduction of the visual field and hemeralopia]. *Confin. Neurol.*, **14**, 184–6.
12. Jacobson,S.G., Cideciyan,A. V., Aleman,T.S., Pianta,M.J., Sumaroka,A., Schwartz,S.B., Smilko,E.E., Milam,A.H., Sheffield,V.C. and Stone,E.M. (2003) Crumbs homolog 1 (CRB1) mutations result in a thick human retina with abnormal lamination. *Hum. Mol. Genet.*, **12**, 1073–1078.
13. Aleman,T.S., Cideciyan,A. V, Aguirre,G.K., Huang,W.C., Mullins,C.L., Roman,A.J., Sumaroka,A., Olivares,M.B., Tsai,F.F., Schwartz,S.B., *et al.* (2011) Human CRB1-associated retinal degeneration: comparison with the rd8 Crb1-mutant mouse model. *Invest. Ophthalmol.*

*Vis. Sci.*, **52**, 6898–910.

14. McKay,G.J., Clarke,S., Davis,J.A., Simpson,D.A.C. and Silvestri,G. (2005) Pigmented paravenous chorioretinal atrophy is associated with a mutation within the crumbs homolog 1 (CRB1) gene. *Invest. Ophthalmol. Vis. Sci.*, **46**, 322–8.
15. Simonelli,F., Ziviello,C., Testa,F., Rossi,S., Fazzi,E., Bianchi,P.E., Fossarello,M., Signorini,S., Bertone,C., Galantuomo,S., *et al.* (2007) Clinical and Molecular Genetics of Leber’s Congenital Amaurosis: A Multicenter Study of Italian Patients. *Investig. Ophthalmology Vis. Sci.*, **48**, 4284.
16. Heckenlively,J.R. (1982) Preserved para-arteriole retinal pigment epithelium (PPRPE) in retinitis pigmentosa. *Br. J. Ophthalmol.*, **66**, 26–30.
17. den Hollander,A.I., Heckenlively,J.R., van den Born,L.I., de Kok,Y.J.M., van der Velde-Visser,S.D., Kellner,U., Jurklies,B., van Schooneveld,M.J., Blankenagel,A., Rohrschneider,K., *et al.* (2001) Leber congenital amaurosis and retinitis pigmentosa with Coats-like exudative vasculopathy are associated with mutations in the crumbs homologue 1 (CRB1) gene. *Am. J. Hum. Genet.*, **69**, 198–203.
18. Vincent,A., Ng,J., Gerth-Kahlert,C., Tavares,E., Maynes,J.T., Wright,T., Tiwari,A., Tumber,A., Li,S., Hanson,J.V.M., *et al.* (2016) Biallelic Mutations in CRB1 Underlie Autosomal Recessive Familial Foveal Retinoschisis. *Invest. Ophthalmol. Vis. Sci.*, **57**, 2637–46.
19. Zenteno,J.C., Buentello-Volante,B., Ayala-Ramirez,R. and Villanueva-Mendoza,C. (2011) Homozygosity mapping identifies the Crumbs homologue 1 (Crb1) gene as responsible for a recessive syndrome of retinitis pigmentosa and nanophthalmos. *Am. J. Med. Genet. A*, **155A**, 1001–6.
20. McMahon,T.T., Kim,L.S., Fishman,G.A., Stone,E.M., Zhao,X.C., Yee,R.W. and Malicki,J. (2009) CRB1 gene mutations are associated with keratoconus in patients with leber congenital amaurosis. *Investig. Ophthalmol. Vis. Sci.*, **50**, 3185–3187.

21. Lotery,A.J., Malik,A., Shami,S.A., Sindhi,M., Chohan,B., Maqbool,C., Moore,P.A., Denton,M.J. and Stone,E.M. (2001) CRB1 mutations may result in retinitis pigmentosa without para-arteriolar RPE preservation. *Ophthalmic Genet.*, **22**, 163–9.
22. Khan KN, Robson A, Mahroo OAR, Gavin Arno, Inglehearn CF, Armengol M, Waseem N, Holder GE, Carss KJ, Raymond LF, Webster AR, Moore AT, McKibbin M, van Genderen MM, Poulter JA,M.M. Clinical and molecular characterisation of CRB1-associated maculopathy. *Eur. Journal Hum. Genet.*, 10.1038/s41431-017-0082-2.
23. Tsang,S.H., Burke,T., Oll,M., Yzer,S., Lee,W., Xie,Y.A. and Allikmets,R. (2014) Whole exome sequencing identifies CRB1 defect in an unusual maculopathy phenotype. *Ophthalmology*, **121**, 1773–82.
24. Bulgakova,N. a and Knust,E. (2009) The Crumbs complex: from epithelial-cell polarity to retinal degeneration. *J. Cell Sci.*, **122**, 2587–96.
25. Bachmann,A., Schneider,M., Theilenberg,E., Grawe,F. and Knust,E. (2001) Drosophila Stardust is a partner of Crumbs in the control of epithelial cell polarity. *Nature*, **414**, 638–43.
26. Lemmers,C., Michel,D., Lane-Guermonprez,L., Delgrossi,M.-H., Médina,E., Arsanto,J.-P. and Le Bivic,A. (2004) CRB3 binds directly to Par6 and regulates the morphogenesis of the tight junctions in mammalian epithelial cells. *Mol. Biol. Cell*, **15**, 1324–33.
27. Roh,M.H., Makarova,O., Liu,C.J., Shin,K., Lee,S., Laurinec,S., Goyal,M., Wiggins,R. and Margolis,B. (2002) The Maguk protein, Pals1, functions as an adapter, linking mammalian homologues of crumbs and discs lost. *J. Cell Biol.*, **157**, 161–172.
28. Alves,C.H., Sanz,A.S., Park,B., Pellissier,L.P., Tanimoto,N., Beck,S.C., Huber,G., Murtaza,M., Richard,F., Sridevi Gurubaran,I., *et al.* (2013) Loss of CRB2 in the mouse retina mimics human retinitis pigmentosa due to mutations in the CRB1 gene. *Hum. Mol. Genet.*, **22**, 35–50.
29. Pellissier,L.P., Alves,C.H., Quinn,P.M., Vos,R.M., Tanimoto,N., Lundvig,D.M.S., Dudok,J.J.,

- Hooibrink,B., Richard,F., Beck,S.C., *et al.* (2013) Targeted ablation of CRB1 and CRB2 in retinal progenitor cells mimics Leber congenital amaurosis. *PLoS Genet.*, **9**, e1003976.
30. van de Pavert,S. a, Kantardzhieva,A., Malysheva,A., Meuleman,J., Versteeg,I., Levelt,C., Klooster,J., Geiger,S., Seeliger,M.W., Rashbass,P., *et al.* (2004) Crumbs homologue 1 is required for maintenance of photoreceptor cell polarization and adhesion during light exposure. *J. Cell Sci.*, **117**, 4169–77.
31. Pellissier,L.P., Lundvig,D.M.S., Tanimoto,N., Klooster,J., Vos,R.M., Richard,F., Sothilingam,V., Garcia Garrido,M., Le Bivic,A., Seeliger,M.W., *et al.* (2014) CRB2 acts as a modifying factor of CRB1-related retinal dystrophies in mice. *Hum. Mol. Genet.*, **23**, 3759–71.
32. van Rossum,A.G.S.H., Aartsen,W.M., Meuleman,J., Klooster,J., Malysheva,A., Versteeg,I., Arsanto,J.-P., Le Bivic,A. and Wijnholds,J. (2006) Pals1/Mpp5 is required for correct localization of Crb1 at the subapical region in polarized Muller glia cells. *Hum. Mol. Genet.*, **15**, 2659–72.
33. Zou,J., Wang,X. and Wei,X. (2012) Crb apical polarity proteins maintain zebrafish retinal cone mosaics via intercellular binding of their extracellular domains. *Dev. Cell*, **22**, 1261–74.
34. Pellissier,L.P., Quinn,P.M., Alves,C.H., Vos,R.M., Klooster,J., Flannery,J.G., Heimel,J.A. and Wijnholds,J. (2015) Gene therapy into photoreceptors and Müller glial cells restores retinal structure and function in CRB1 retinitis pigmentosa mouse models. *Hum. Mol. Genet.*, **24**, 3104–18.
35. den Hollander,A.I., Ghiani,M., de Kok,Y.J.M., Wijnholds,J., Ballabio,A., Cremers,F.P.M. and Broccoli,V. (2002) Isolation of Crb1, a mouse homologue of Drosophila crumbs, and analysis of its expression pattern in eye and brain. *Mech. Dev.*, **110**, 203–207.
36. Alves,C.H., Pellissier,L.P. and Wijnholds,J. (2014) The CRB1 and adherens junction complex proteins in retinal development and maintenance. *Prog. Retin. Eye Res.*, **40**, 35–52.

37. van de Pavert,S.A., Sanz,A.S., Aartsen,W.M., Vos,R.M., Versteeg,I., Beck,S.C., Klooster,J., Seeliger,M.W. and Wijnholds,J. (2007) Crb1 is a determinant of retinal apical Müller glia cell features. *Glia*, **55**, 1486–97.
38. van de Pavert,S. a, Meuleman,J., Malysheva,A., Aartsen,W.M., Versteeg,I., Tonagel,F., Kamphuis,W., McCabe,C.J., Seeliger,M.W. and Wijnholds,J. (2007) A single amino acid substitution (Cys249Trp) in Crb1 causes retinal degeneration and deregulates expression of pituitary tumor transforming gene Pttg1. *J. Neurosci.*, **27**, 564–73.
39. Alves,C.H., Pellissier,L.P., Vos,R.M., Garcia Garrido,M., Sothilingam,V., Seide,C., Beck,S.C., Klooster,J., Furukawa,T., Flannery,J.G., *et al.* (2014) Targeted ablation of Crb2 in photoreceptor cells induces retinitis pigmentosa. *Hum. Mol. Genet.*, **23**, 3384–401.
40. Zhao,M., Andrieu-Soler,C., Kowalczyk,L., Paz Cortés,M., Berdugo,M., Dernigoghossian,M., Halili,F., Jeanny,J.-C., Goldenberg,B., Savoldelli,M., *et al.* (2015) A new CRB1 rat mutation links Müller glial cells to retinal telangiectasia. *J. Neurosci.*, **35**, 6093–106.
41. Mehalow,A.K., Kameya,S., Smith,R.S., Hawes,N.L., Denegre,J.M., Young,J. a, Bechtold,L., Haider,N.B., Tepass,U., Heckenlively,J.R., *et al.* (2003) CRB1 is essential for external limiting membrane integrity and photoreceptor morphogenesis in the mammalian retina. *Hum. Mol. Genet.*, **12**, 2179–89.
42. Alves,C.H., Bossers,K., Vos,R.M., Essing,A.H.W., Swagemakers,S., van der Spek,P.J., Verhaagen,J. and Wijnholds,J. (2013) Microarray and Morphological Analysis of Early Postnatal CRB2 Mutant Retinas on a Pure C57BL/6J Genetic Background. *PLoS One*, **8**, e82532.
43. Dudok,J.J., Sanz,A.S., Lundvig,D.M.S., Sothilingam,V., Garrido,M.G., Klooster,J., Seeliger,M.W. and Wijnholds,J. (2013) MPP3 regulates levels of PALS1 and adhesion between photoreceptors and Müller cells. *Glia*, **61**, 1629–44.
44. Park,B., Alves,C.H., Lundvig,D.M., Tanimoto,N., Beck,S.C., Huber,G., Richard,F., Klooster,J.,

- Andlauer,T.F.M., Swindell,E.C., *et al.* (2011) PALS1 is essential for retinal pigment epithelium structure and neural retina stratification. *J. Neurosci.*, **31**, 17230–41.
45. Bujakowska,K., Audo,I., Mohand-Saïd,S., Lancelot,M.-E., Antonio,A., Germain,A., Lèveillard,T., Letexier,M., Saraiva,J.-P., Lonjou,C., *et al.* (2012) CRB1 mutations in inherited retinal dystrophies. *Hum. Mutat.*, **33**, 306–15.
46. Koike,C., Nishida,A., Akimoto,K., Nakaya,M., Noda,T., Ohno,S. and Furukawa,T. (2005) Function of atypical protein kinase C lambda in differentiating photoreceptors is required for proper lamination of mouse retina. *J. Neurosci.*, **25**, 10290–8.
47. Park,R., Moon,U.Y., Park,J.Y., Hughes,L.J., Johnson,R.L., Cho,S.-H. and Kim,S. (2016) Yap is required for ependymal integrity and is suppressed in LPA-induced hydrocephalus. *Nat. Commun.*, **7**, 10329.
48. Zhao,L., Zabel,M.K., Wang,X., Ma,W., Shah,P., Fariss,R.N., Qian,H., Parkhurst,C.N., Gan,W.-B. and Wong,W.T. (2015) Microglial phagocytosis of living photoreceptors contributes to inherited retinal degeneration. *EMBO Mol. Med.*, **7**, 1179–1197.
49. Aartsen,W.M., Kantardzhieva,A., Klooster,J., van Rossum,A.G.S.H., van de Pavert,S.A., Versteeg,I., Cardozo,B.N., Tonagel,F., Beck,S.C., Tanimoto,N., *et al.* (2006) Mpp4 recruits Psd95 and Veli3 towards the photoreceptor synapse. *Hum. Mol. Genet.*, **15**, 1291–1302.
50. Stöhr,H., Heisig,J.B., Benz,P.M., Schöberl,S., Milenkovic,V.M., Strauss,O., Aartsen,W.M., Wijnholds,J., Weber,B.H.F. and Schulz,H.L. (2009) TMEM16B, a novel protein with calcium-dependent chloride channel activity, associates with a presynaptic protein complex in photoreceptor terminals. *J. Neurosci.*, **29**, 6809–18.
51. Nishida,A., Furukawa,A., Koike,C., Tano,Y., Aizawa,S., Matsuo,I. and Furukawa,T. (2003) Otx2 homeobox gene controls retinal photoreceptor cell fate and pineal gland development. *Nat. Neurosci.*, **6**, 1255–63.

52. Quinn,P.M., Buck,T.M., Alves,C., Ohonin,C., Chuva de Sousa Lopes,S.M., Mikkers,H.M.M. and Wijnbolds,J. (2017) Recapitulation of the Human Fetal Crumbs Complex in human iPSCs-derived Retinas and Retinal Pigment Epithelium. *Invest. Ophthalmol. Vis. Sci.*, **58(8)**, 3758.
53. Jacobson,S.G., Cideciyan,A. V., Aleman,T.S., Pianta,M.J., Sumaroka,A., Schwartz,S.B., Smilko,E.E., Milam,A.H., Sheffield,V.C. and Stone,E.M. (2003) Crumbs homolog 1 (CRB1) mutations result in a thick human retina with abnormal lamination. *Hum. Mol. Genet.*, **12**, 1073–8.
54. Yzer,S., Fishman,G.A., Racine,J., Al-Zuhaibi,S., Chakor,H., Dorfman,A., Szlyk,J., Lachapelle,P., Van Den Born,L.I., Allikmets,R., *et al.* (2006) CRB1 heterozygotes with regional retinal dysfunction: Implications for genetic testing of leber congenital amaurosis. *Investig. Ophthalmol. Vis. Sci.*, **47**, 3736–3744.
55. Nishiguchi,K.M., Carvalho,L.S., Rizzi,M., Powell,K., Holthaus,S.-M.K., Azam,S. a., Duran,Y., Ribeiro,J., Luhmann,U.F.O., Bainbridge,J.W.B., *et al.* (2015) Gene therapy restores vision in rd1 mice after removal of a confounding mutation in Gpr179. *Nat. Commun.*, **6**, 6006.
56. Tanimoto,N., Sothilingam,V., Kondo,M., Biel,M., Humphries,P. and Seeliger,M.W. (2015) Electroretinographic assessment of rod- and cone-mediated bipolar cell pathways using flicker stimuli in mice. *Sci. Rep.*, **5**, 10731.
57. Tanimoto,N., Akula,J.D., Fulton,A.B., Weber,B.H.F. and Seeliger,M.W. (2016) Differentiation of murine models of ‘negative ERG’ by single and repetitive light stimuli. *Doc. Ophthalmol.*, **132**, 101–109.
58. Klooster,J. and Kamermans,M. (2016) An ultrastructural and immunohistochemical analysis of the outer plexiform layer of the retina of the European silver eel (*Anguilla anguilla* L). *PLoS One*, **11**, 1–21.

## Legends to Figures

**Figure 1:** Progressive loss of retinal function in  $Crb1^{KO}Crb2^{Low-imPRC}$  mice. Electroretinographic analysis of 1-, 3-, 6-6-month(s) old control (black) and  $Crb1^{KO}Crb2^{Low-imPRC}$  affected mice (blue). **(A)** Scotopic and photopic single-flash intensity series from representative animals at 1-month of age. The control scotopic a-wave is indicated by the open arrow and the black arrow points to the attenuated a-wave of the  $Crb1^{KO}Crb2^{Low-imPRC}$ . **(B)** Quantitative evaluation of scotopic single-flash b-wave, a-wave amplitudes ( $1.5 \log \text{cd s/m}^2$ ) and the corresponding b-wave/a-wave amplitude ratio (b/a ratio). **(C, D, and E)** Time course single-flash ERG data from 1- (left), 3- (middle) and 6- (right) months-old mice. Scotopic (SC) a-wave **(C)** and scotopic and photopic (PH) b-wave amplitudes **(D and E, respectively)** plotted as a function of the logarithm of the flash intensity. **(F)** Time course of flicker response amplitudes from 1- (left), 3- (middle) and 6- (right) months-old mice. Boxes indicate the 25 and 75% quantile range and whiskers indicate the 5 and 95% quantiles, and the intersection of line and error bar indicates the median of the data (box-and-whisker plot). Number of animals used: 1-month-old (1M): seven controls and four  $Crb1^{KO}Crb2^{Low-imPRC}$ ; 3M: five controls and four  $Crb1^{KO}Crb2^{Low-imPRC}$ ; 6M: four per group.

**Fig 2:** Removal of CRB1 from Müller glial cells and reduction of CRB2 from photoreceptors leads to abnormal layering and ONL thinning. Toluidine-stained light microscopy of retinal sections from control (A, D and G) and  $Crb1^{KO}Crb2^{Low-imPRC}$  mice superior (B, E, and H) and inferior (C, F and I), at different ages, (A-C) – 1M, (D-F) – 3M, (G-I) – 6M. In the superior  $Crb1^{KO}Crb2^{Low-imPRC}$  retina at 1-, 3-, and 6M of age, disruptions of the OLM, and protrusions of photoreceptor nuclei into the inner- and outer segment layer (arrows), and ingressions of nuclei from the ONL into the OPL (arrowheads) are observed (B, E, and H). In the inferior  $Crb1^{KO}Crb2^{Low-imPRC}$  retina at 1M half rosettes in the ONL (arrowhead) and protrusions of INL cells into the ONL (arrow) are observed (C). In the inferior retina at 3M, there is thinning of the ONL (arrow) (F). At 3M and 6M there are areas with no ONL (arrowheads) (F and I). Quantification of ONL thickness in  $Crb1^{KO}Crb2^{Low-imPRC}$  mice at 1mm from the ONH showed significant thickening (P10, P14, and 1M) and thinning (3M) of the inferior versus

the superior and control retina (J). Total retina thickness at 6M was significantly thinner in the inferior versus superior and control retina (K). GCL, ganglion cell layer; INL, inner nuclear layer; ONL, outer nuclear layer; RPE, retinal pigment epithelium; ONH, optic nerve head; OPL, outer plexiform layer. Scale bar: (A–I) 20  $\mu$ m. Data are presented as mean  $\pm$  SEM; n = 3–4, per timepoint. \* $p$  < 0.05; \*\* $P$  < 0.01, \*\*\*  $p$  < 0.001.

**Fig 3:** Maintenance of CRB complex in the adult  $Crb1^{KO}Crb2^{Low-imPRC}$  superior retina. CRB Complex in 3M  $Crb1^{KO}Crb2^{Low-imPRC}$  mice. Immunohistochemistry pictures from (3M) retina sections stained for subapical region markers (red): CRB2 (A-C), PALS1 (D-F), MUPP1 (G-I) and for adherens junction markers (green): p120-catenin (A-C), N-cadherin (D-F). Disruptions of adherens junction markers were detected in both superior (B, E, H) and inferior (C, F, I)  $Crb1^{KO}Crb2^{Low-imPRC}$  retina. Ectopic photoreceptor nuclei protruded into the inner- and outer segment layer in the superior  $Crb1^{KO}Crb2^{Low-imPRC}$  retina near the ONH where there were disruptions of subapical region markers (B, E, H). Inferior  $Crb1^{KO}Crb2^{Low-imPRC}$  retina showed loss of subapical region markers at phenotype foci but maintenance most peripherally. (C, F, I). A thickened apical OLM was positive for adherens junction markers in the inferior  $Crb1^{KO}Crb2^{Low-imPRC}$  retina at phenotype foci. OLM, outer limiting membrane; ONL, outer nuclear layer. Scale bar: 20  $\mu$ m.

**Fig 4:** Neovascularization, gliosis, and microglia activation due to lack of CRB1 in Müller glial cells and a decrease of CRB2 in photoreceptors. Immunohistochemistry of 3-month-old  $Crb1^{KO}Crb2^{Low-imPRC}$  mouse retinas. Sections were stained with antibodies against: SOX9 and glutamine synthetase (GS) (A-C), GFAP (D-F), CD45 and vWF (G-I), CD11b and IB4 (J-L). In the  $Crb1^{KO}Crb2^{Low-imPRC}$  retinas, SOX9-positive Müller glial cell nuclei were misplaced into the ONL both in the superior and inferior retina (arrows) (B and C). Arrowheads indicate the SOX9-positive nuclei in retinal pigment epithelium. The  $Crb1^{KO}Crb2^{Low-imPRC}$  mutant retinas showed activated Müller glia cells, detected by an increase in the GFAP staining, more strongly inferiorly than superiorly (E and F). Activated apical processes were seen wrapping the OLM around photoreceptors (arrows) or INL cells (arrowhead) (E and F). An increase in microglial and endothelial cell markers in the ONL is observed more strongly

inferiorly than superiorly in *Crb1<sup>KO</sup>Crb2<sup>Low-imPRC</sup>* retinas (H, I, K and L). CD45 and vWF ~~primarily~~ colocalised (inserts) being found more basally in the superior ONL and throughout the ONL inferiorly (H and I). CD11b was found to be expressed in the ONL (boxed area) or partially overlapped with IB4 (arrow) (K and L). GCL, ganglion cell layer; INL, inner nuclear layer; ONL, outer nuclear layer; OLM, outer limiting membrane. Scale bars: (A-L) 20  $\mu$ m, inserts in (H, I, K and L) 10  $\mu$ m.

**Fig 5:** Reduction of CRB2 in photoreceptors and ablation of CRB1 from Müller glial cells leads to a disruption of synapses and degeneration of the photoreceptors. Immunohistochemistry of 3-month-old *Crb1<sup>KO</sup>Crb2<sup>Low-imPRC</sup>* mouse retinas. Sections were stained with antibodies against: Tuj1 and recoverin (A-C), rhodopsin and cone arrestin (D-F), S-opsin and PNA (G-I), PKC $\alpha$  and MPP4 (J-L). Recoverin positive cells localised to the ONL in Control (A) and superior *Crb1<sup>KO</sup>Crb2<sup>Low-imPRC</sup>* mouse retinas (B). Recoverin can also mark ON-bipolar cells, (asterisks, B). At foci in the inferior retina few photoreceptors remained and no longer had segments (C). Tuj1 ~~normally localised~~ localised normally to ganglion cells and dendrites in the superior *Crb1<sup>KO</sup>Crb2<sup>Low-imPRC</sup>* retina but could be found in breaks of the ONL/INL inferiorly (insert) (B and C). The *Crb1<sup>KO</sup>Crb2<sup>Low-imPRC</sup>* retina superiorly showed ectopic cones at basal positions (insert), and inferiorly at foci, few cones remained while ectopic rhodopsin expression was found in the cell soma (insert) (E and F). Superior and inferior *Crb1<sup>KO</sup>Crb2<sup>Low-imPRC</sup>* retina had ectopic S-opsin localised in the cell soma (inserts) (H and I). Mislocalised PNA positive staining was seen at foci of S-opsin internalisation superiorly and throughout the ONL, INL, and GCL inferiorly (H and I). MPP4 was found mislocalised in the ONL, minorly superiorly and throughout degenerated foci inferiorly (inserts) (K and L). Protruding bipolar cell dendrites ~~could be~~ were found in the ONL inferiorly (arrow) (L). GCL, ganglion cell layer; INL, inner nuclear layer; ONL, outer nuclear layer; OLM, outer limiting membrane. Scale bars: (A-L) 20  $\mu$ m, inserts in (H, I, K and L) 10  $\mu$ m.

**Fig 6:** Severe and early retinal disorganisation in *Crb1<sup>KO</sup>Crb2<sup>ΔimPRC</sup>* mice. Toluidine-stained light microscopy of retinal sections from control (A, D, and G), superior (B, E, H) and inferior (C, F, I)

*Crb1<sup>KO</sup>Crb2<sup>ΔimPRC</sup>* mice (at different ages, (A-C) – E17.5, (D-F, L) – P1, (G-I, M) – P5. Overview stitches of superior–inferior asymmetry in P1 and P5 *Crb1<sup>KO</sup>Crb2<sup>ΔimPRC</sup>* retina (L and M, respectively). In the *Crb1<sup>KO</sup>Crb2<sup>ΔimPRC</sup>* retina from E17.5 ectopic nuclei ~~could be were~~ found in the GCL (B and C, arrows). At E17 and P1 intact outer limiting membrane is still present inferiorly (C and F, arrowheads). In P1 and P5 retina rosettes were found in the NL (E, F, and H, asterisk) and at P5 no separate ONL and OPL formed (H and I). Electron microscopic pictures of the subapical region of retinal progenitor cells at E17.5 in control (J) and *Crb1<sup>KO</sup>Crb2<sup>ΔimPRC</sup>* retinas (K). In the control retina, the adherens junctions were regularly distributed and aligned (J, arrowheads), and correct arrangement of photoreceptor inner segments ~~were~~ detected. In the *Crb1<sup>KO</sup>Crb2<sup>ΔimPRC</sup>* retina, adherens junctions and inner segments were not observed (K). GCL, ganglion cell layer; INL, inner nuclear layer; ONL, outer nuclear layer; ONH, optic nerve head; NL, nuclear layer; NBL, neuroblast layer; μ, microvilli; IS, inner segment; PRC, photoreceptor cell. Scale bars: (A–I) 20 μm, (J and K) 1 μm.

**Fig 7:** Peripheral inferior maintenance of CRB complex at the subapical region in ~~the~~ early postnatal *Crb1<sup>KO</sup>Crb2<sup>ΔimPRC</sup>* retina. Immunohistochemistry pictures from (P1) retina sections stained for subapical region markers (red): CRB2 (A-C), PAR3 (D-F), PALS1 (G-I), MUPP1 (J-L) and for adherens junction markers (green): p120-catenin (A-C), β-catenin (D-F), N-cadherin (G-I). Disruptions of adherens junction markers were detected in both superior (B, E, H, K) and inferior (C, F, I, L) *Crb1<sup>KO</sup>Crb2<sup>ΔimPRC</sup>* retina. Subapical region markers were mislocalised into the NBL in the superior *Crb1<sup>KO</sup>Crb2<sup>ΔimPRC</sup>* retina (B, E, H, K). In the inferior *Crb1<sup>KO</sup>Crb2<sup>ΔimPRC</sup>* peripheral retina subapical region and adherens junction markers were found correctly localised in sections (C, F, I, L). Ectopic photoreceptor nuclei protruded into the inner- and outer segment layer in the inferior *Crb1<sup>KO</sup>Crb2<sup>ΔimPRC</sup>* retina (C and L). OLM, outer limiting membrane; NBL, neuroblast layer. Scale bar: 20 μm.

**Fig 8:** Lack of CRB2 from postmitotic photoreceptors and CRB1 from radial glial progenitors affects apoptosis and mitosis. Immunohistochemistry of P1 control (A and D), and *Crb1<sup>KO</sup>Crb2<sup>ΔimPRC</sup>*

superior (B and E) and inferior (C and F) mouse retinas. Sections were stained with antibodies against: Ki67 and pH3 (A-C), Recoverin (D-F). Quantification of pH3- (G), Ki67- (H) and cCaspase3-positive cells (I). Mislocalised pH3-positive dividing cells and Ki67-positive cycling cells were detected in the bottom nuclear layer (bNL) and the GCL with an increase in total positive cells at P1 in *Crb1<sup>KO</sup>Crb2<sup>ΔimPRC</sup>* retina (B, C, arrowheads; quantifications G and H). Ectopic recoverin positive post mitotic photoreceptors were found throughout the *Crb1<sup>KO</sup>Crb2<sup>ΔimPRC</sup>* retina (E and F, arrowheads). A significant increase in total apoptotic cells was found in *Crb1<sup>KO</sup>Crb2<sup>ΔimPRC</sup>* retina at P1 (I). GCL, ganglion cell layer; NBL, neuroblast layer; tNL, top nuclear layer; bNL, bottom nuclear layer. Scale bar: (A–F) 20 μm. Data are presented as mean ± SEM; n = 3–4 retina, per genotype. \**p* < 0.05; \*\* *p* < 0.01, \*\*\* *p* < 0.001.

**Fig 9: Conditional disruption of one or both alleles of *Crb2* in immature photoreceptors, on a genetic background lacking *Crb1*, Loss of full or half levels of CRB2 in photoreceptors with concomitant loss of CRB1 in Müller glial cells** leads to superior-inferior asymmetry. Toluidine-stained light microscopy showing retinal stitiches (A-C) and superior (A', B' and C') and inferior (A'', B'' and C'') inserts from control (A, A' and A''), *Crb1<sup>KO</sup>Crb2<sup>Low-imPRC</sup>* (B, B' and B'') and *Crb1<sup>KO</sup>Crb2<sup>ΔimPRC</sup>* (C, C' and C'') mice, at P14. *Crb1<sup>KO</sup>Crb2<sup>Low-imPRC</sup>* retinas show an inferior phenotype of half rosettes in the ONL that ingressed into the INL at foci and ectopic photoreceptor nuclei that protruded into the inner- and outer segment layer (B and B''). *Crb1<sup>KO</sup>Crb2<sup>ΔimPRC</sup>* retina exhibit a superior and inferior phenotype with apical rosettes, a single mixed nuclear layer abutting the retinal pigment epithelium and ectopic photoreceptors in the GCL (C, C' and C''). A significant increase in superior and inferior GCL thickness was found in *Crb1<sup>KO</sup>Crb2<sup>ΔimPRC</sup>* retina (D). GCL thickness was found to be extended further from the ONH superiorly than inferiorly. Quantification of recoverin-positive photoreceptor cells showed their mislocalisation into the bNL and GCL of *Crb1<sup>KO</sup>Crb2<sup>ΔimPRC</sup>* retina compared to *Crb1<sup>KO</sup>Crb2<sup>Low-imPRC</sup>* and control retina (E). A significantly higher amount of recoverin-positive photoreceptor cells wereas found in the superior compared to the inferior *Crb1<sup>KO</sup>Crb2<sup>ΔimPRC</sup>* retina (F). GCL, ganglion cell layer; INL, inner nuclear layer; ONL, outer nuclear layer; RPE, retinal pigment epithelium; ONH, optic nerve head; NL, nuclear layer. Scale bar: (A', A'', B', B'', C' and C'') 20

$\mu\text{m}$ . Data are presented as mean  $\pm$  SEM; n = 3–4 retinae, per genotype. \*  $p < 0.05$ ; \*\*  $p < 0.01$ , \*\*\*  $p < 0.001$ .

**Supplemental Fig 1:** Graphical schematic of the localisation of CRB1 and CRB2 in radial glial progenitor cells (RGPC), Müller glial cells (MG), Rod and Cone photoreceptor cells in wild-type, *Crbl<sup>KO</sup>Crb2<sup>F/F</sup>* (Control), *Crbl<sup>KO</sup>Crb2<sup>Low-imPRC</sup>*, and *Crbl<sup>KO</sup>Crb2 <sup>$\Delta$ imPRC</sup>* mice.

**Supplemental Fig 2:** Reduced Mendelian ratio, survival, and body weight in *Crbl<sup>KO</sup>Crb2 <sup>$\Delta$ imPRC</sup>* mice with hydrocephalus. Lower than the predicted Mendelian ratio of *Crbl<sup>KO</sup>Crb2 <sup>$\Delta$ imPRC</sup>* mice (A). Reduced percent survival of *Crbl<sup>KO</sup>Crb2 <sup>$\Delta$ imPRC</sup>* mice compared to *Crbl<sup>KO</sup>Crb2<sup>Low-imPRC</sup>* and control mice (B). *Crbl<sup>KO</sup>Crb2 <sup>$\Delta$ imPRC</sup>* mice unable to sustain their body weight compared to *Crbl<sup>KO</sup>Crb2<sup>Low-imPRC</sup>* and control mice (C). Picture of P14 control, *Crbl<sup>KO</sup>Crb2<sup>Low-imPRC</sup>*, and *Crbl<sup>KO</sup>Crb2 <sup>$\Delta$ imPRC</sup>* mice. *Crbl<sup>KO</sup>Crb2 <sup>$\Delta$ imPRC</sup>* mouse has hydrocephalus.

**Supplemental Fig 3:** Abnormal layering and superior/inferior asymmetry in adult *Crbl<sup>KO</sup>Crb2<sup>Low-imPRC</sup>* mice. Toluidine-stained light microscopy (A). (A–D). Peripheral inferior retina phenotype transition in *Crbl<sup>KO</sup>Crb2<sup>Low-imPRC</sup>* mice at 1-, 3-, and 6-months of age (A–C, respectively). Retinal stitch of 1M *Crbl<sup>KO</sup>Crb2 <sup>$\Delta$ imPRC</sup>* mouse retina showing superior- inferior asymmetry (A). (D). GCL, ganglion cell layer; INL, inner nuclear layer; ONL, outer nuclear layer; ONH, optic nerve head. Scale bar: (A–C) 20  $\mu\text{m}$ .

**Supplemental Fig 4:** Abnormal layering and superior/inferior asymmetry in aged *Crbl<sup>KO</sup>Crb2<sup>Low-imPRC</sup>* mice. Toluidine-stained light microscopy (A, B). Toluidine-stained light microscopy (A, B). Retinal stitch of 3M and 6M *Crbl<sup>KO</sup>Crb2 <sup>$\Delta$ imPRC</sup>* mouse retina showing superior- inferior asymmetry (A and B, respectively).

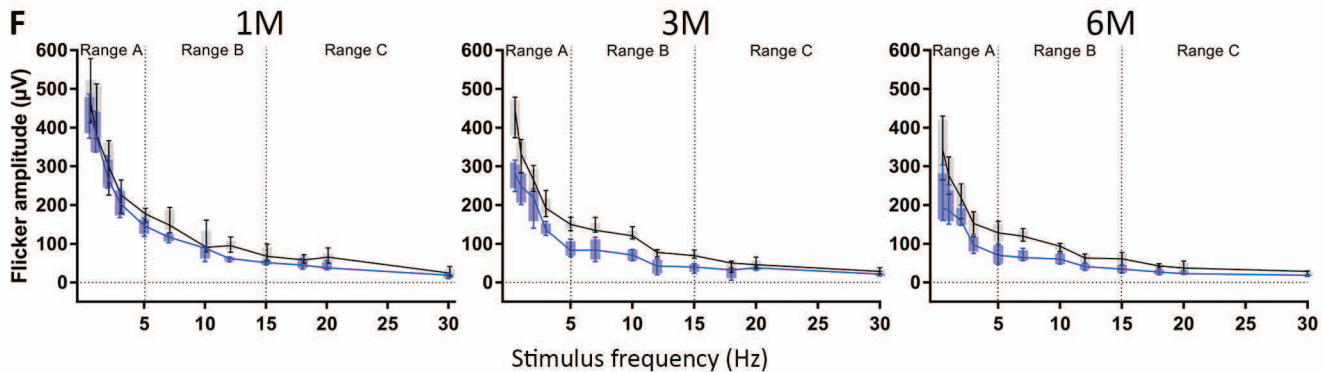
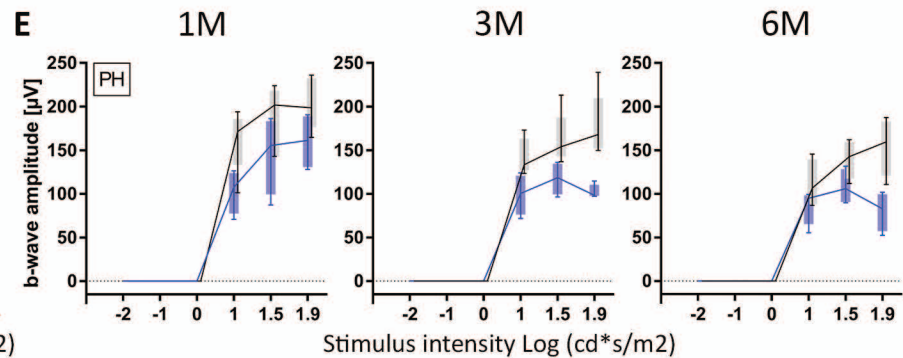
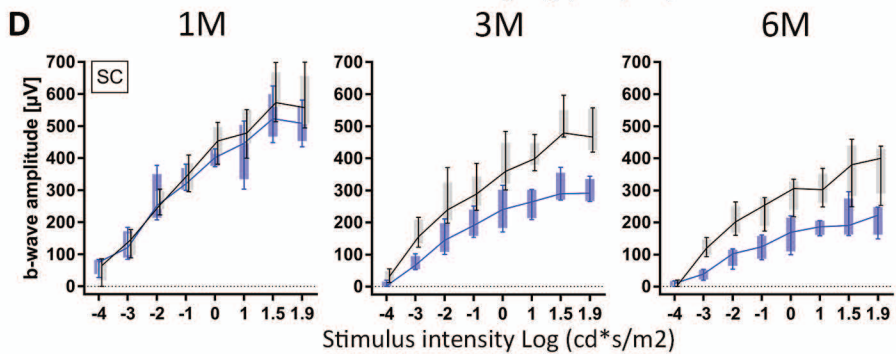
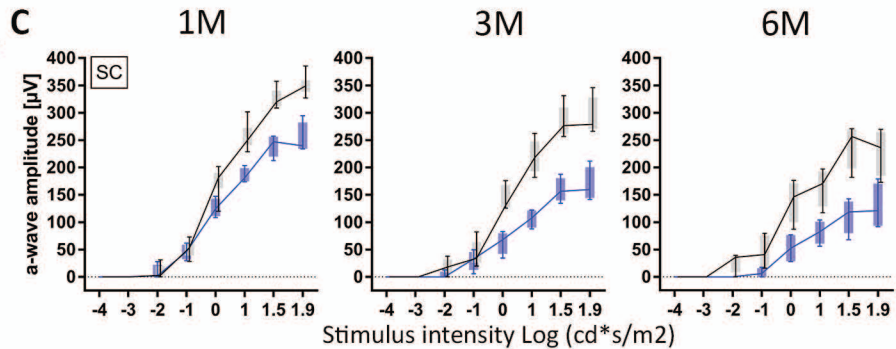
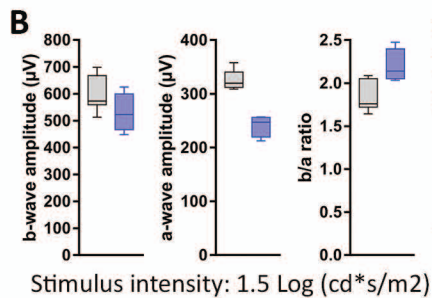
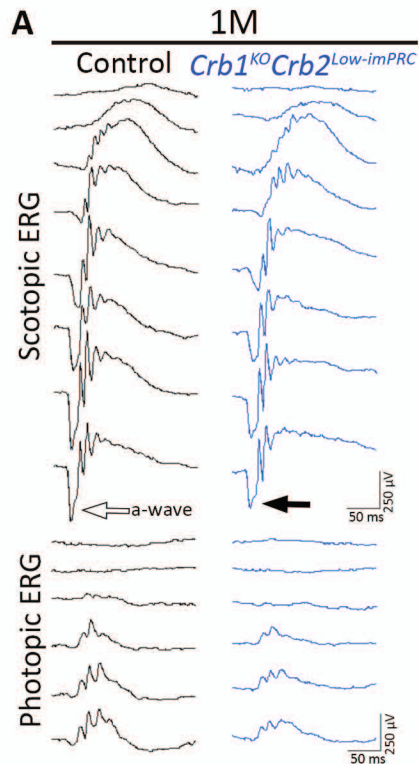
**Supplemental Fig 5:** Peripheral inferior retina phenotype transition in *Crbl<sup>KO</sup>Crb2<sup>Low-imPRC</sup>* mice. Toluidine-stained light microscopy (A, B). Peripheral inferior retina phenotype transition in

*Crb1<sup>KO</sup>Crb2<sup>Low-imPRC</sup>* mice at 1-, 3-, and 6-months of age (A-C, respectively). GCL, ganglion cell layer; INL, inner nuclear layer; ONL, outer nuclear layer; ONH, optic nerve head. Scale bar: (A–C) 20  $\mu$ m.

**Supplemental Fig 46:** Increase in cleaved Caspase-3 positive cells in early postnatal *Crb1<sup>KO</sup>Crb2 <sup>$\Delta$ imPRC</sup>* mice. Immunohistochemistry of cleaved Caspase-3 (cCasp3) positive apoptotic cells. Positive cells were found localised throughout the retina. Significantly more apoptotic cells were found in *Crb1<sup>KO</sup>Crb2 <sup>$\Delta$ imPRC</sup>* retina at P1 (Fig. 8I). GCL, ganglion cell layer; NBL, neuroblast layer. Scale bar: 20  $\mu$ m.

**Supplemental Fig 57:** Ectopic photoreceptors in ganglion cell layer of *Crb1<sup>KO</sup>Crb2 <sup>$\Delta$ imPRC</sup>* mice. Recoverin (Red) and rhodopsin (Green) positive photoreceptor cells localise to the ONL in control (A) and *Crb1<sup>KO</sup>Crb2<sup>Low-imPRC</sup>* (B) mice. Photoreceptors were found ectopically in the GCL in the superior (C) and inferior (D) retina of *Crb1<sup>KO</sup>Crb2 <sup>$\Delta$ imPRC</sup>* mice. GCL, ganglion cell layer; INL, inner nuclear layer; ONL, outer nuclear layer; NL, nuclear layer. Scale bar: 20  $\mu$ m.

**Supplemental Fig 86:** Defects in retinal vasculature in *Crb1<sup>KO</sup>Crb2 <sup>$\Delta$ imPRC</sup>* and *Crb1<sup>KO</sup>Crb2<sup>Low-imPRC</sup>* mice. In control retina, Griffonia simplicifolia B4-isolectin (IB4, Red) stains for retinal vasculature and is restricted to the inner retina (A). In *Crb1<sup>KO</sup>Crb2<sup>Low-imPRC</sup>* mice, ectopic IB4 staining is found in rosettes of the ONL (B). In the Superior (C) and Inferior (D), *Crb1<sup>KO</sup>Crb2 <sup>$\Delta$ imPRC</sup>* retina IB4 is found mislocalised to the NL. GCL, ganglion cell layer; INL, inner nuclear layer; ONL, outer nuclear layer; NL, nuclear layer. Scale bar: 20  $\mu$ m.

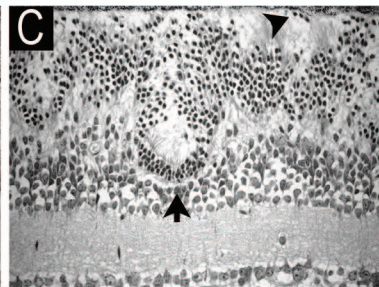
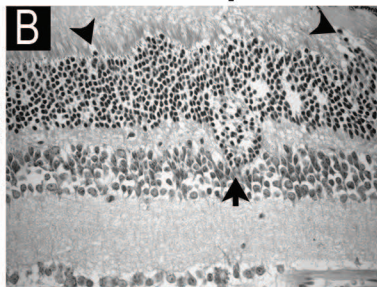
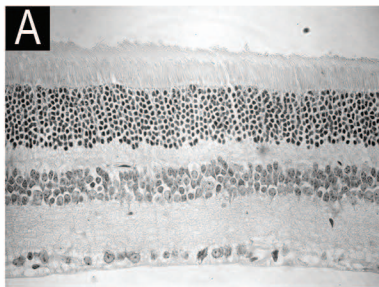


CONTROL

ONH-Superior

Inferior

1M

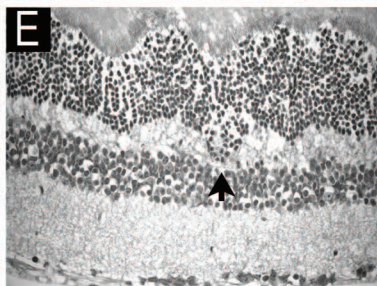
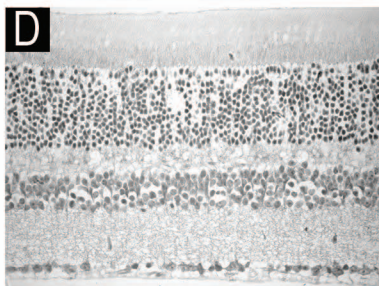


ONL

INL

GCL

3M

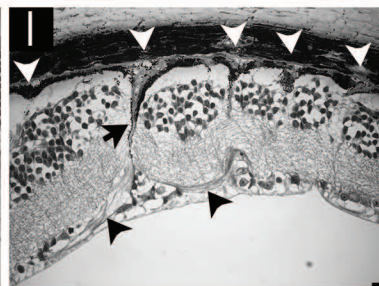
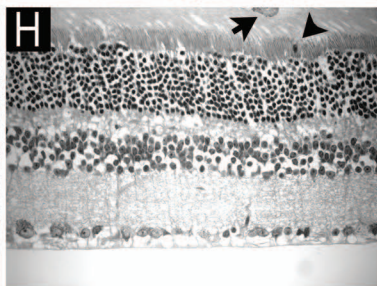
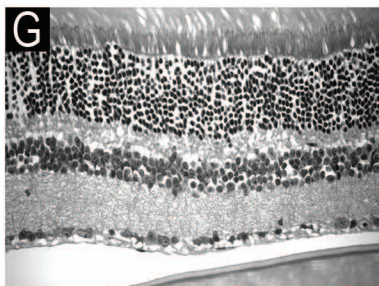


ONL

INL

GCL

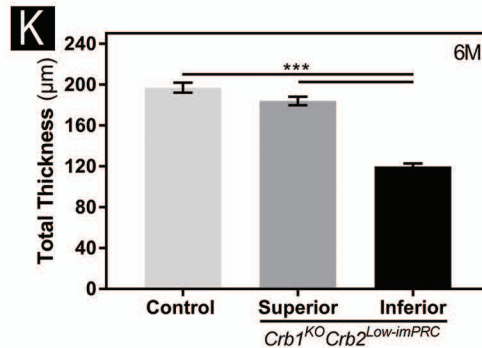
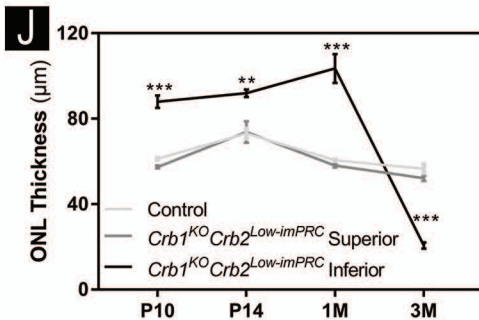
6M



RPE

INL

GCL

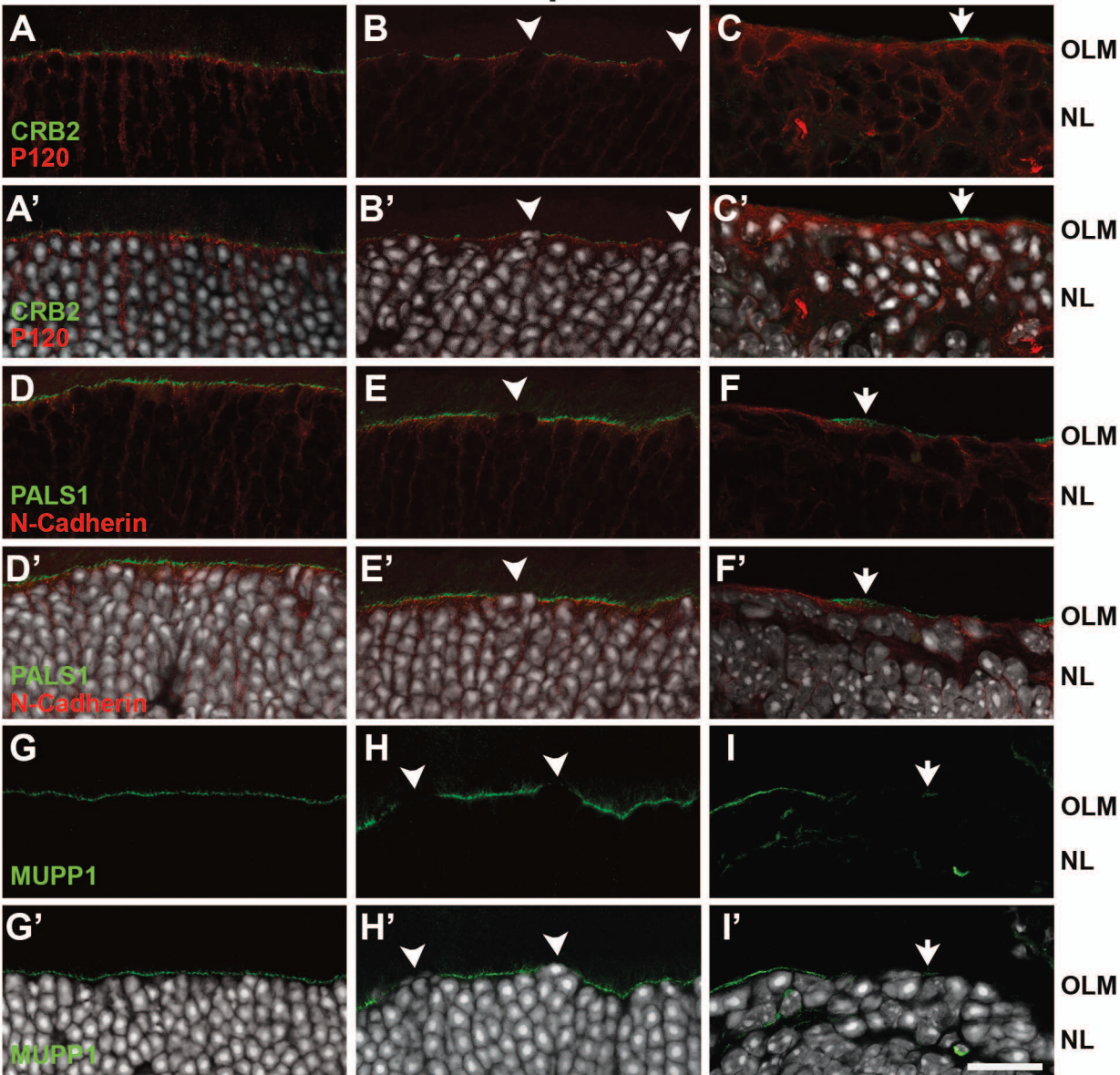


*Crb1*<sup>KO</sup> *Crb2*<sup>Low-imPRC</sup>

Control

ONH-Superior

Inferior

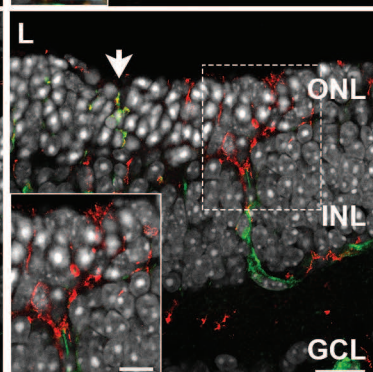
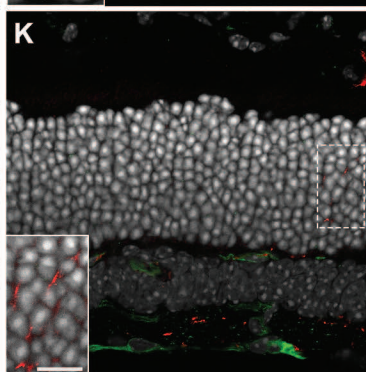
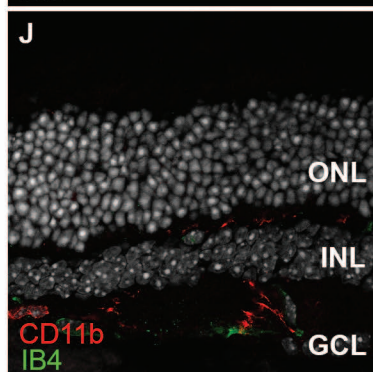
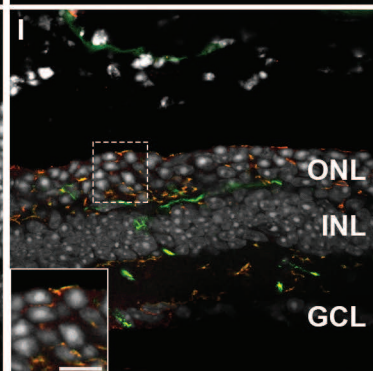
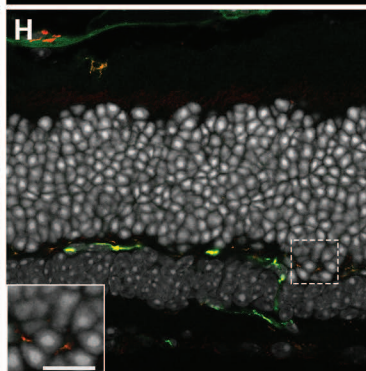
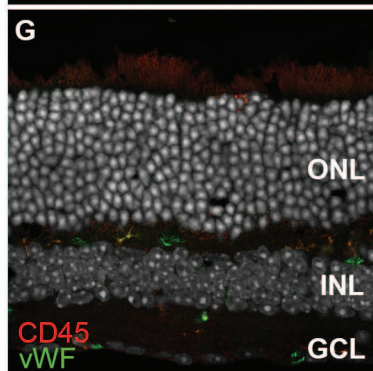
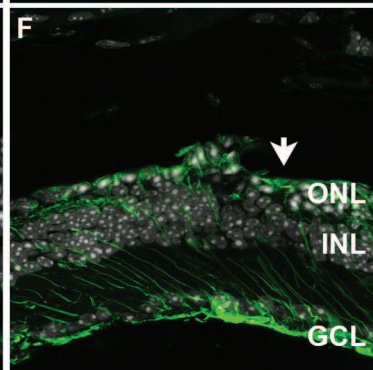
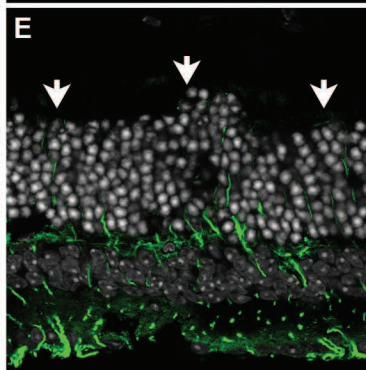
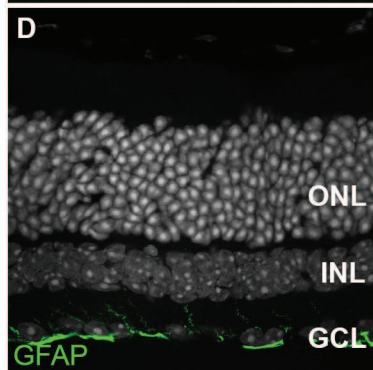
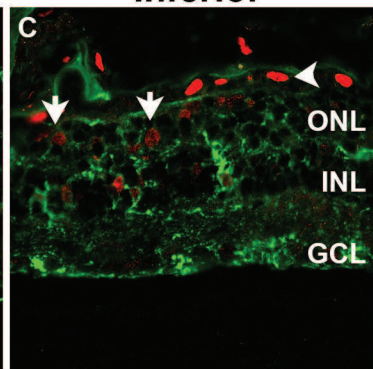
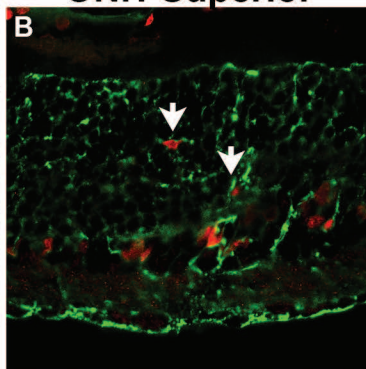
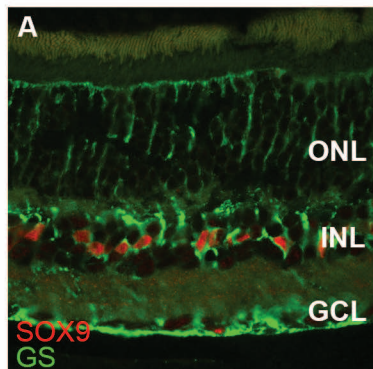


**CONTROL**

***Crb1*<sup>KO</sup> *Crb2*<sup>Low-imPRC</sup>**

**ONH-Superior**

**Inferior**

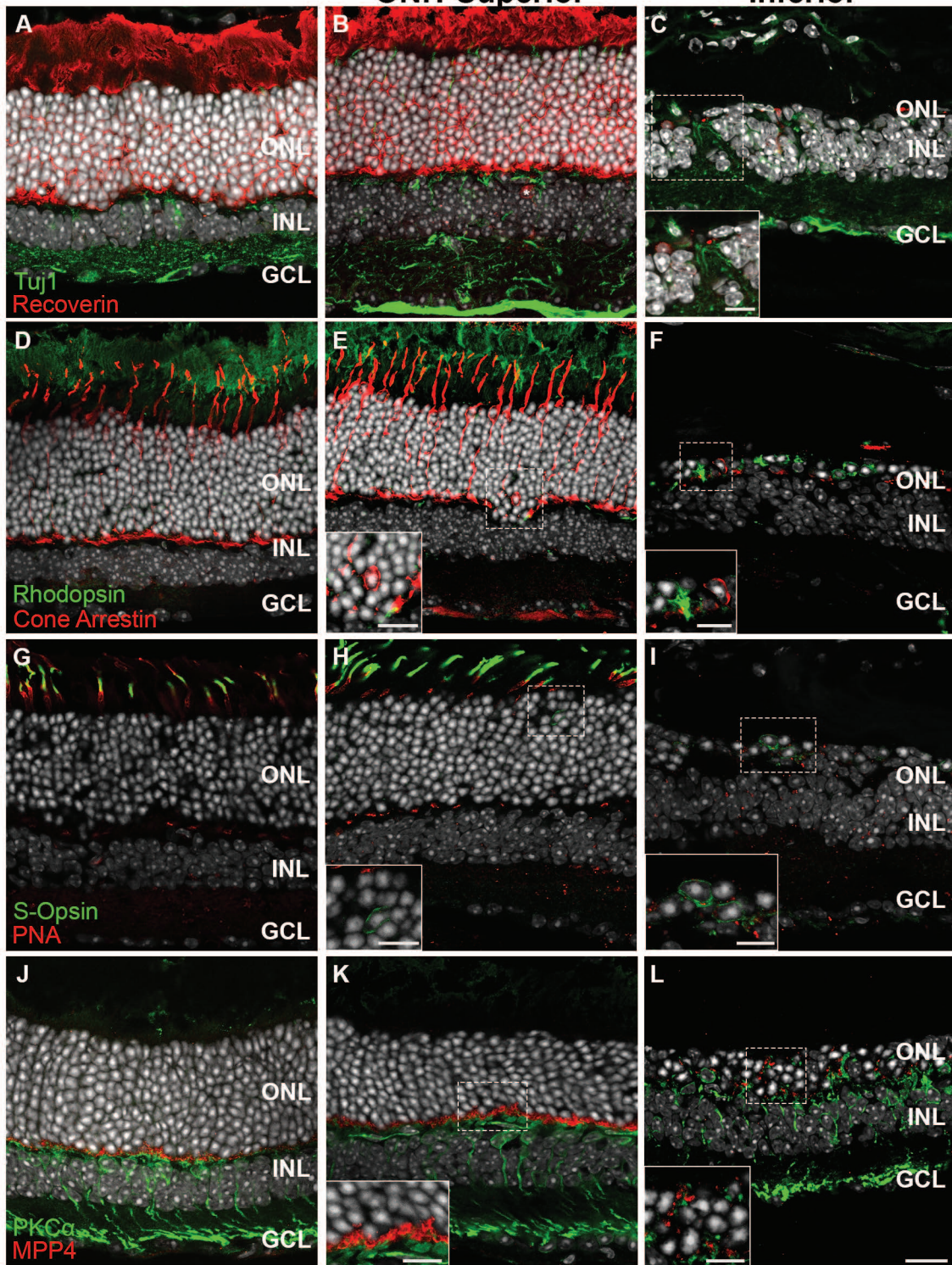


# CONTROL

*Crb1*<sup>KO</sup> *Crb2*<sup>Low-imPRC</sup>

# ONH-Superior

# Inferior



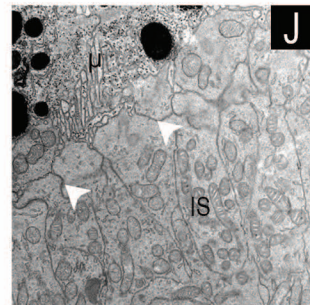
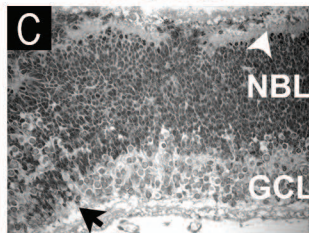
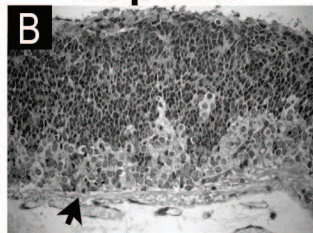
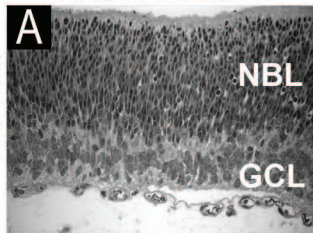
*Crb1*<sup>KO</sup> *Crb2*<sup>ΔimPRC</sup>

CONTROL

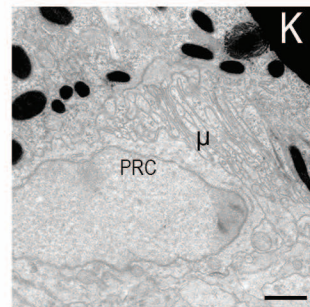
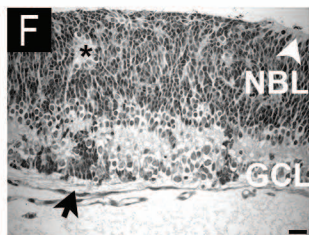
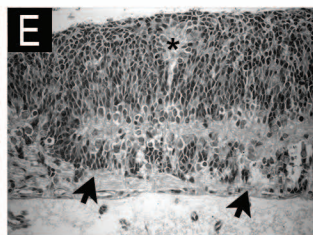
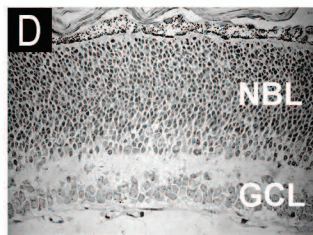
Superior

Inferior

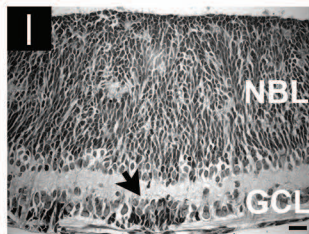
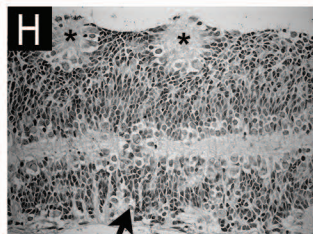
E17.5



P1

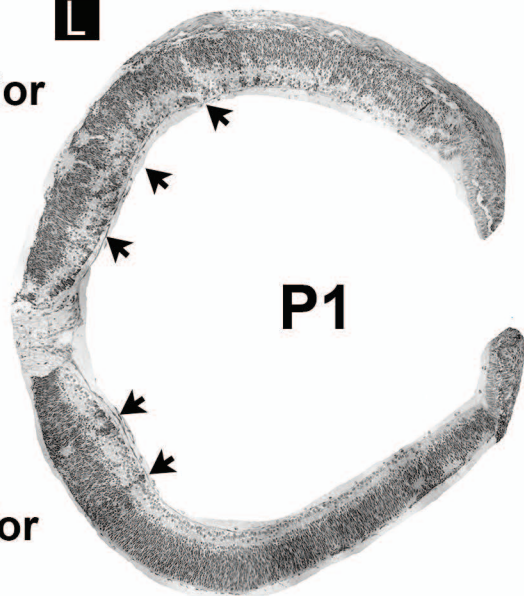


P5



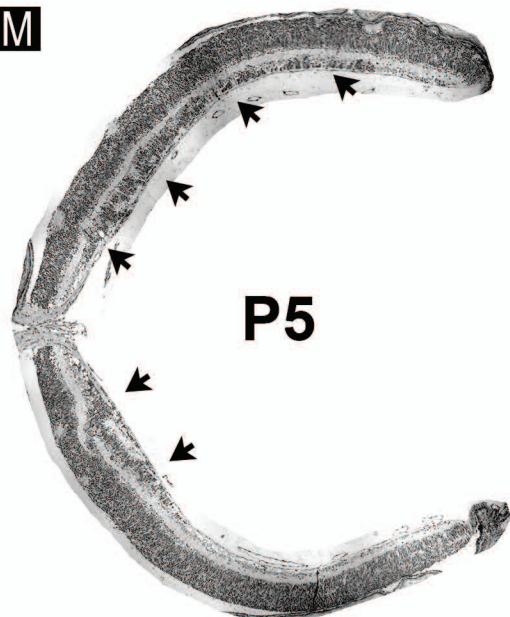
**L**

Superior



Inferior

**M**

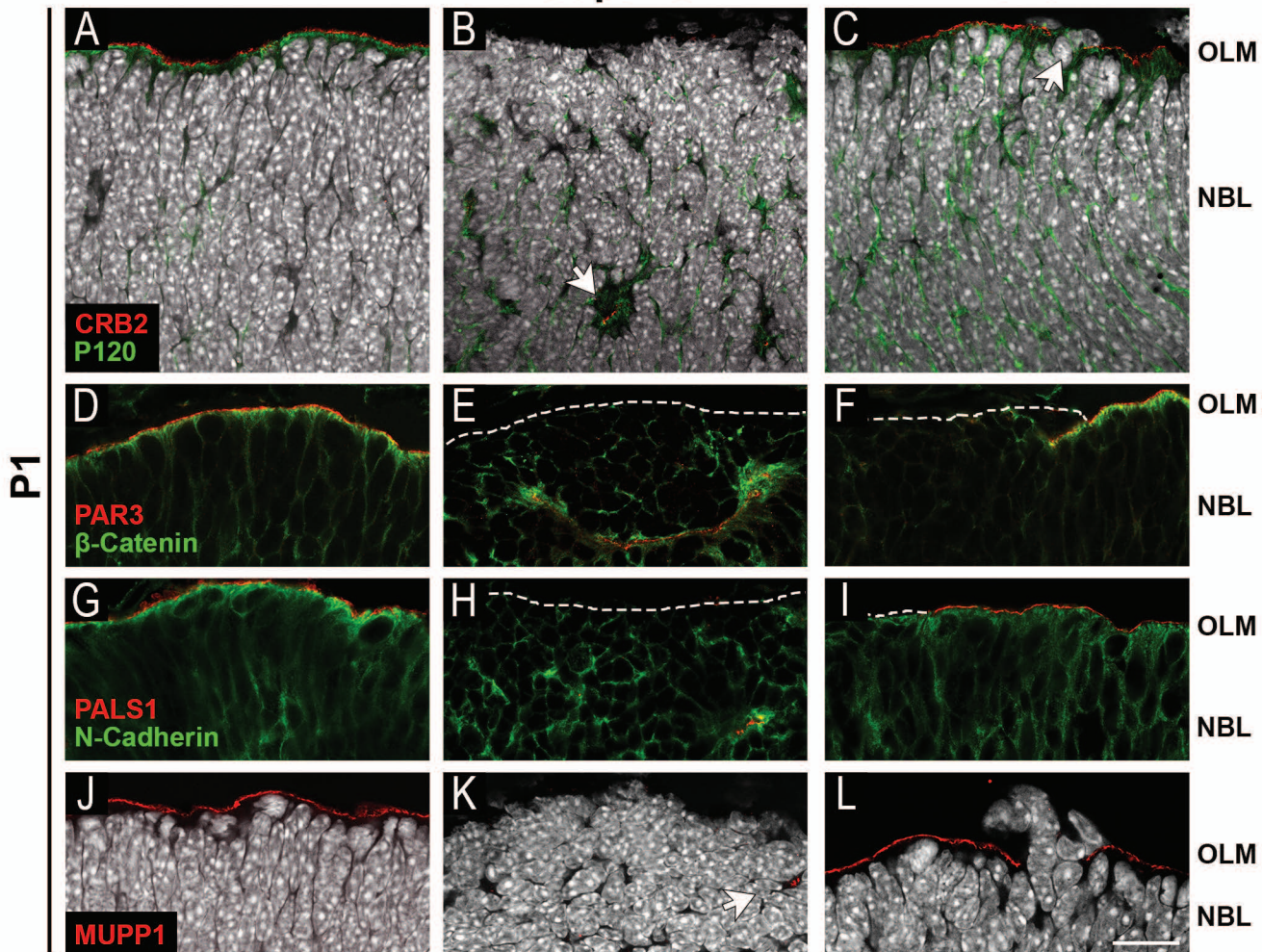


*Crb1*<sup>KO</sup>*Crb2*<sup>ΔimPRC</sup>

CONTROL

Superior

Inferior

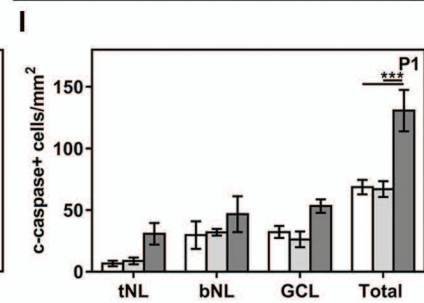
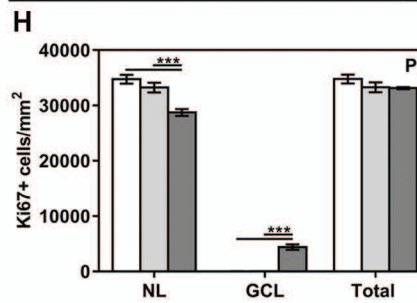
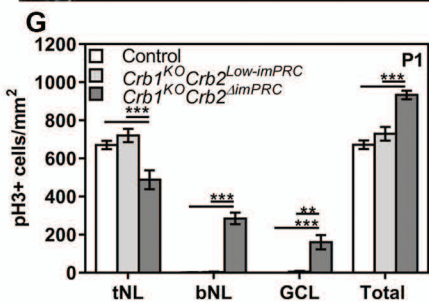
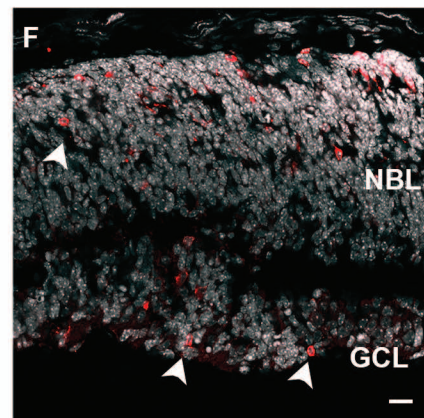
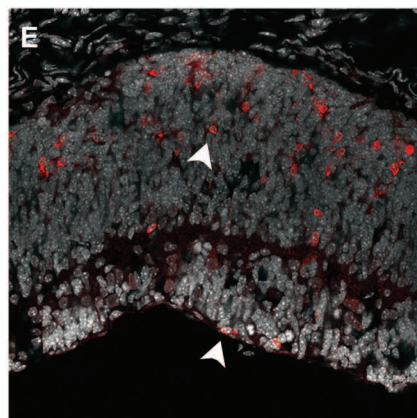
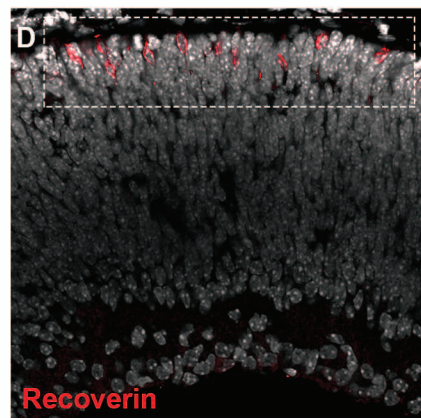
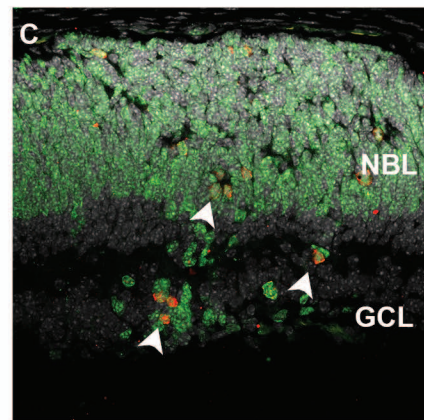
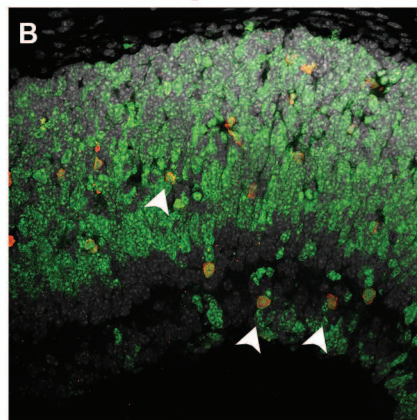
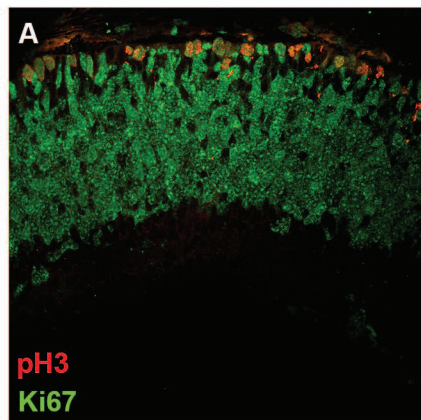


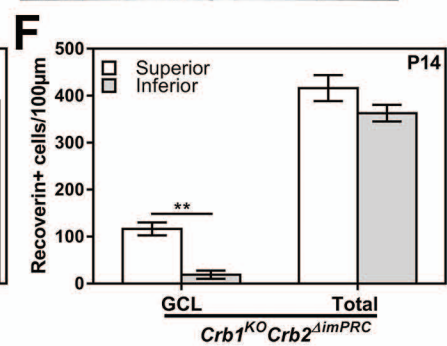
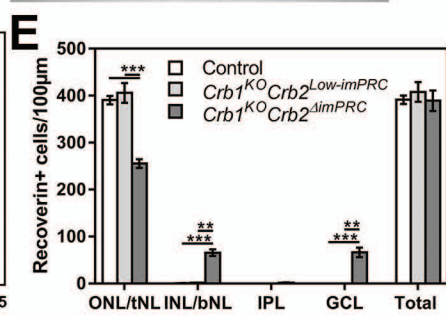
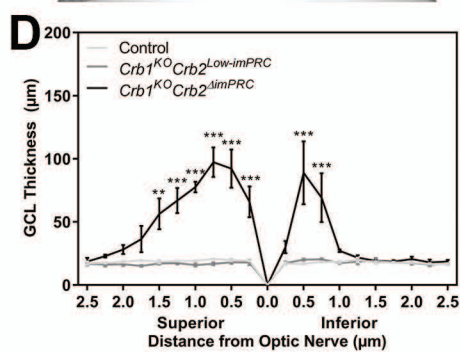
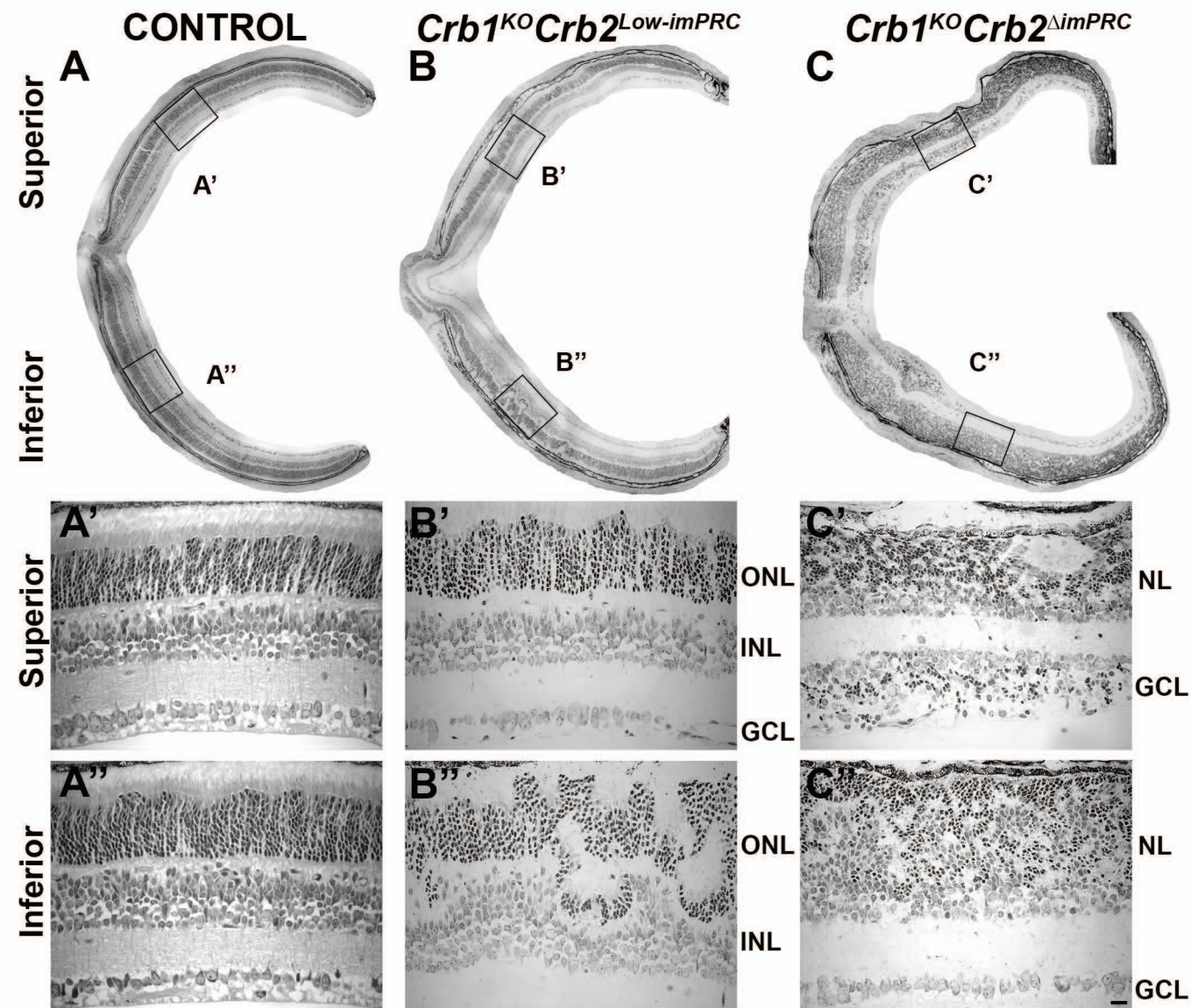
*Crb1*<sup>KO</sup>*Crb2*<sup>ΔimPRC</sup>

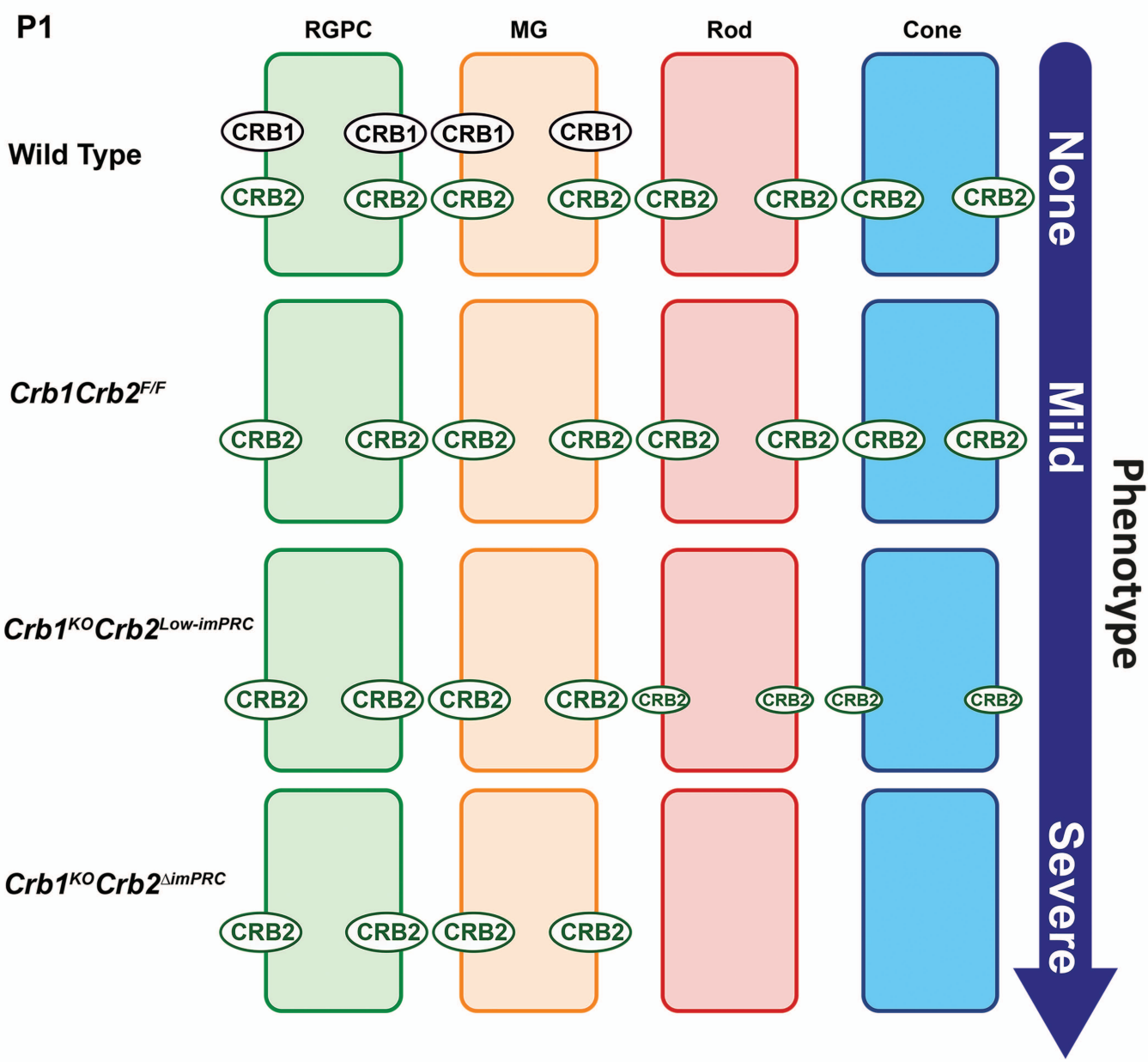
CONTROL

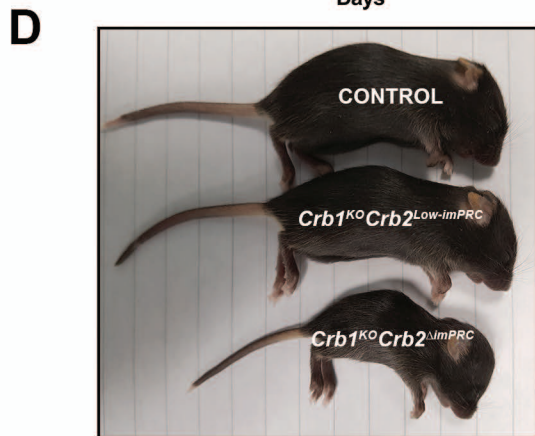
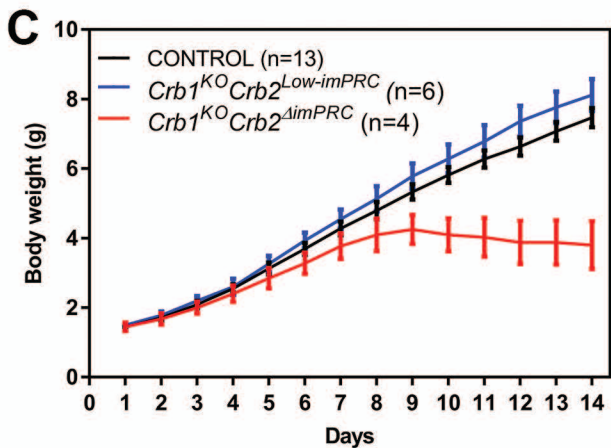
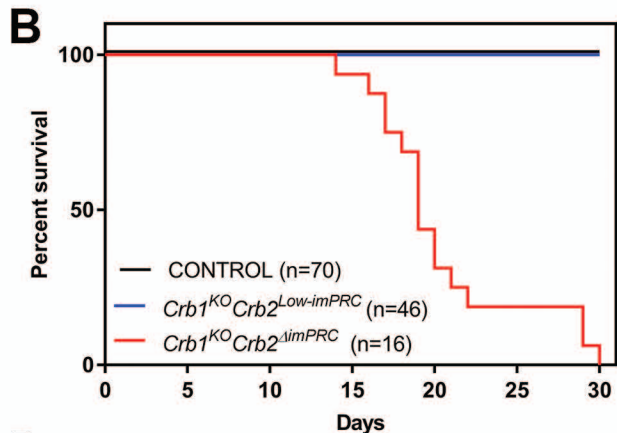
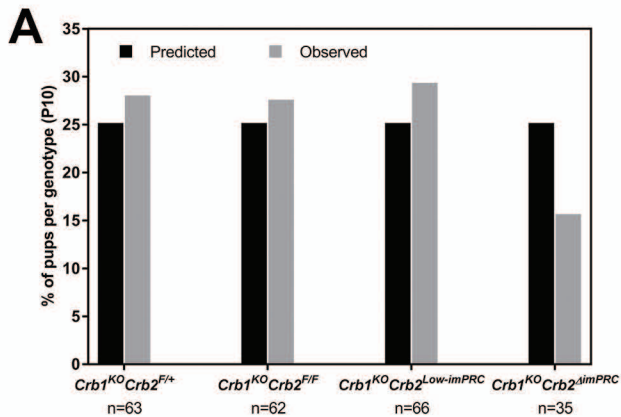
Superior

Inferior





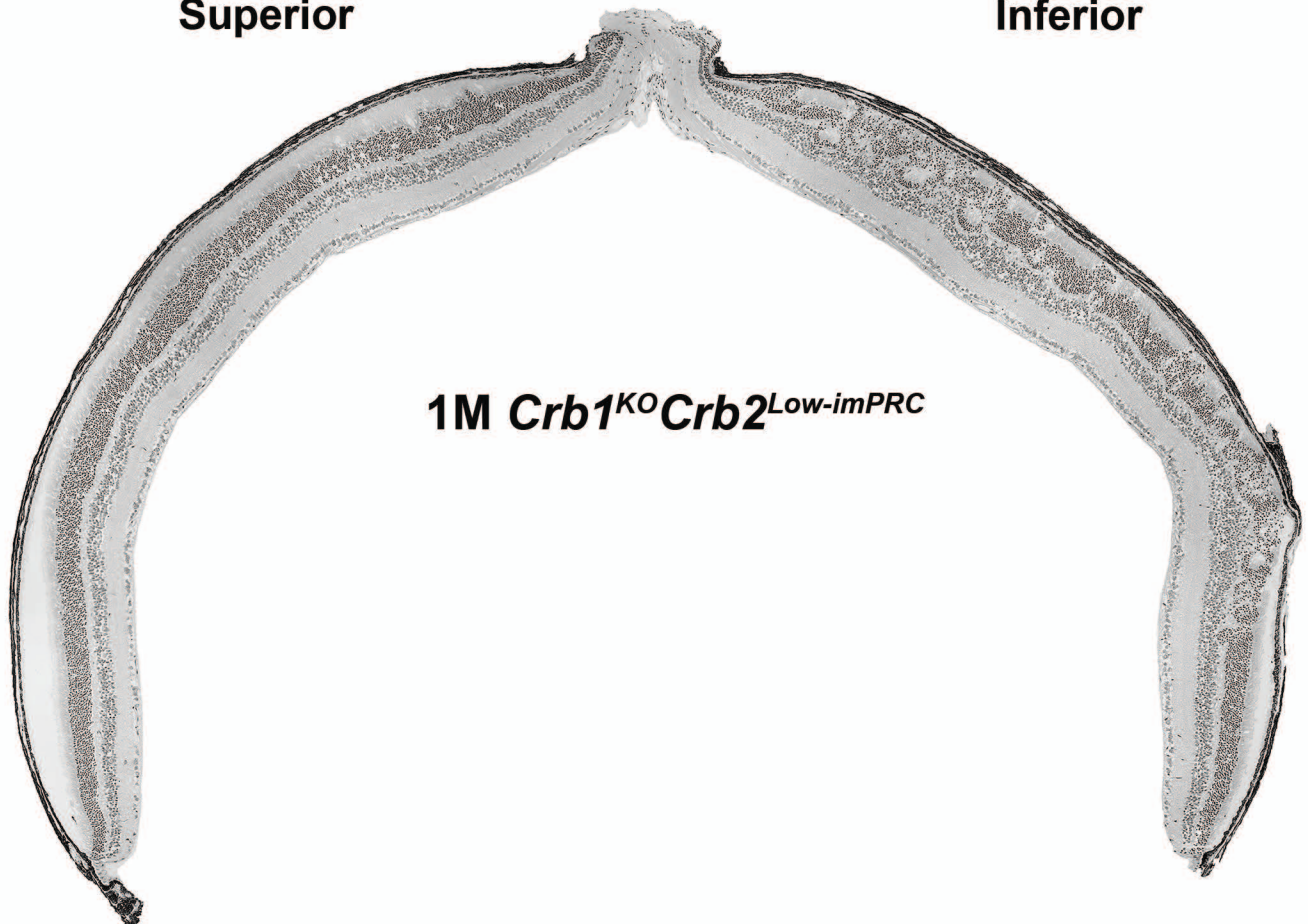




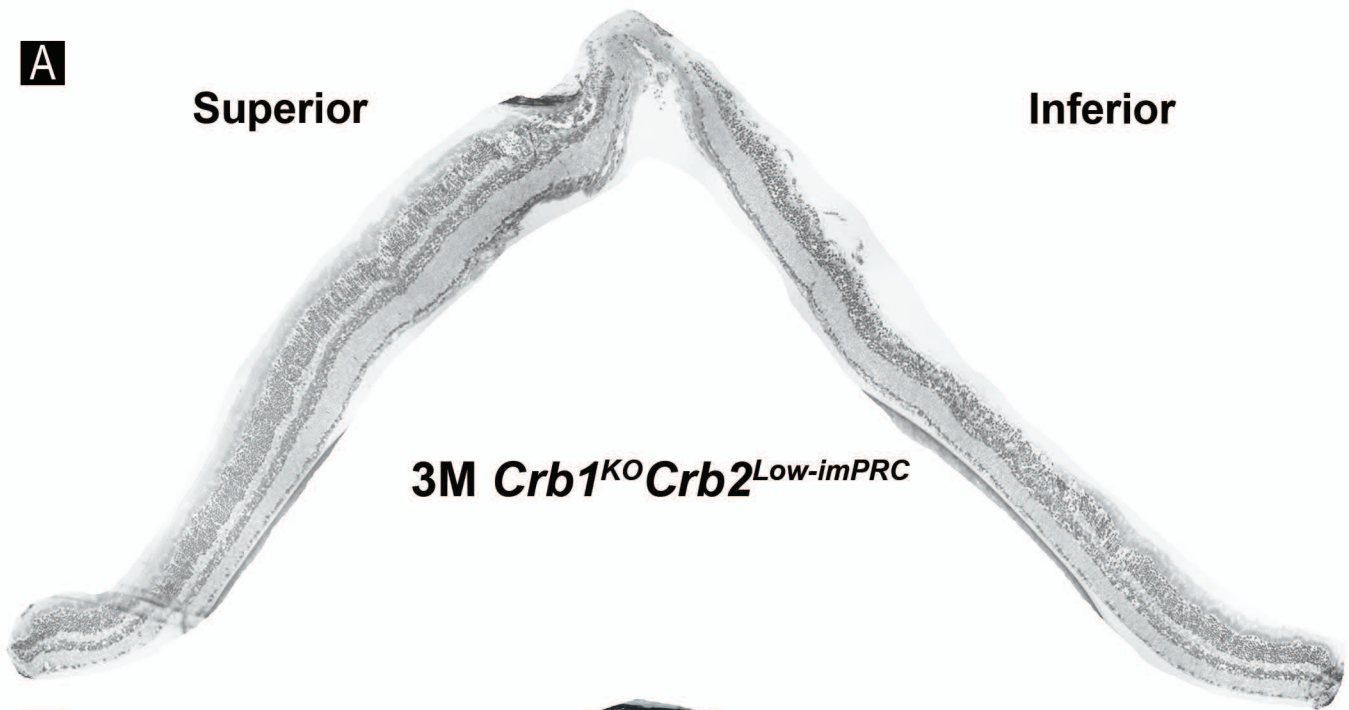
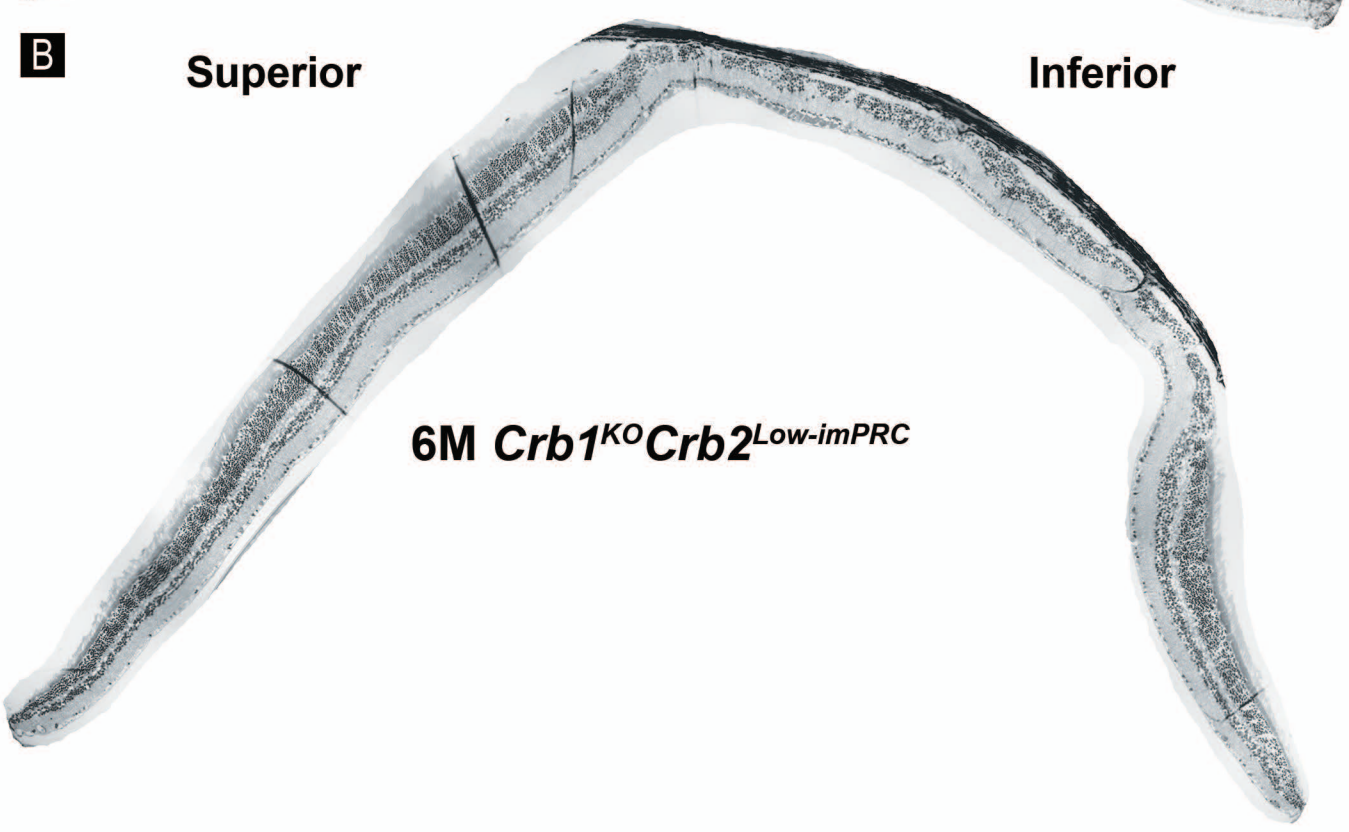
**A**

**Superior**

**Inferior**



**1M *Crb1*<sup>KO</sup> *Crb2*<sup>Low-imPRC</sup>**

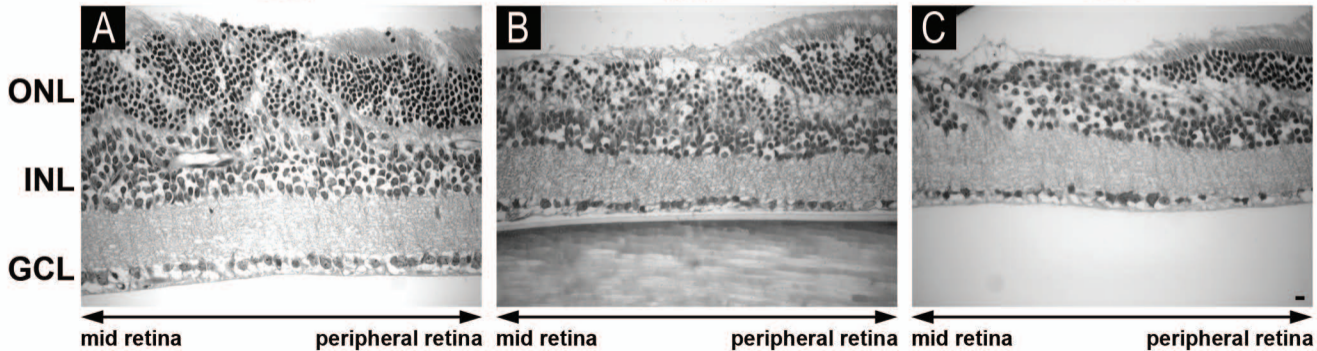
**A****Superior****Inferior****3M *Crb1*<sup>KO</sup>*Crb2*<sup>Low-imPRC</sup>****B****Superior****Inferior****6M *Crb1*<sup>KO</sup>*Crb2*<sup>Low-imPRC</sup>**

# *Crb1*<sup>KO</sup>*Crb2*<sup>Low-imPRC</sup> peripheral inferior retina

1M

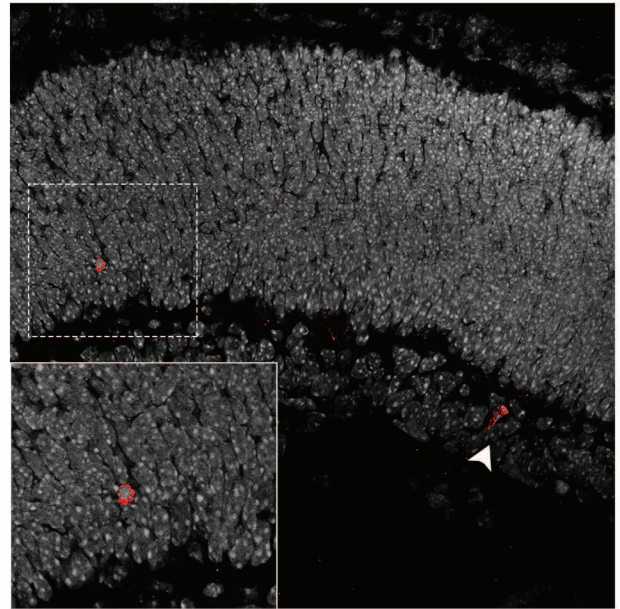
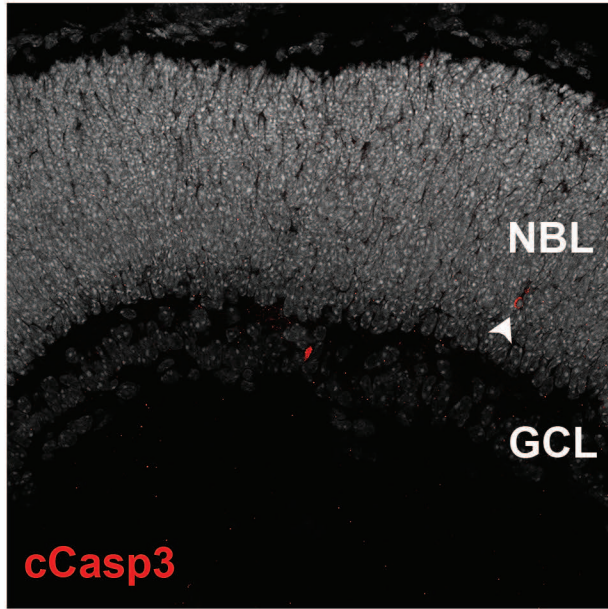
3M

6M



**CONTROL**

***Crb1*<sup>KO</sup>*Crb2*<sup>Low-imPRC</sup>**

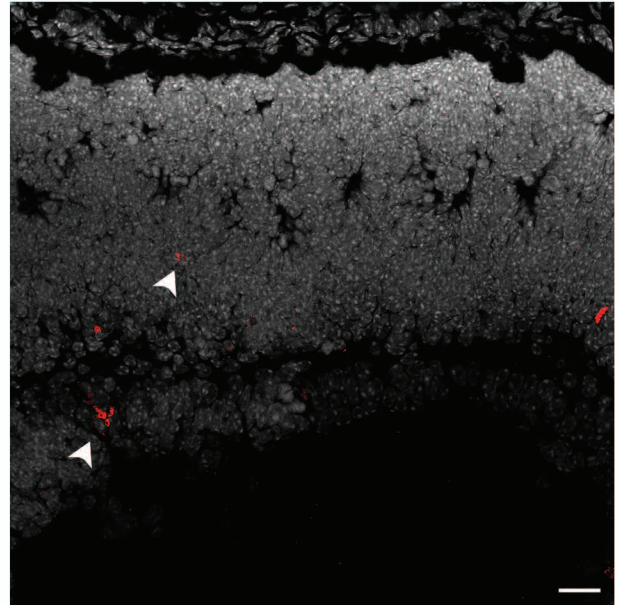
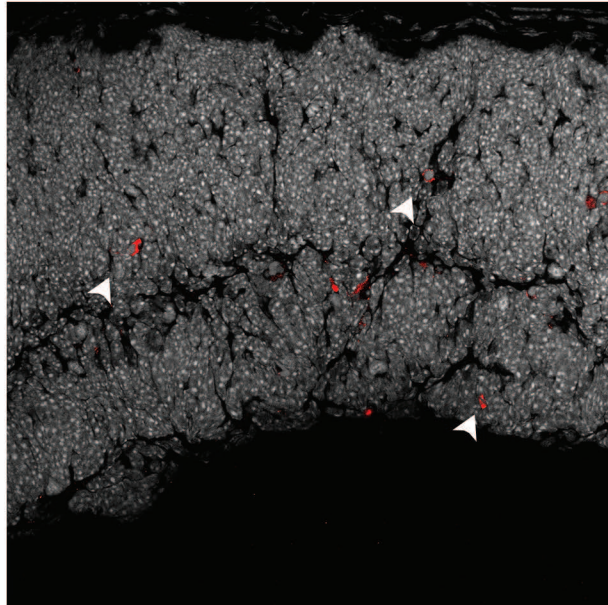


**P1**

***Crb1*<sup>KO</sup>*Crb2*<sup>ΔimPRC</sup>**

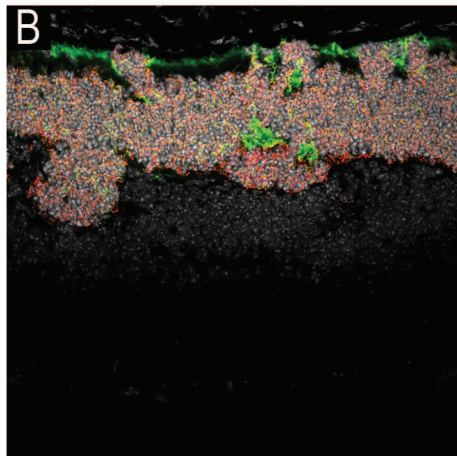
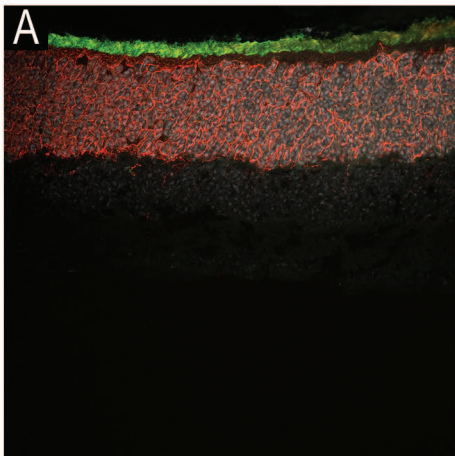
**Superior**

**Inferior**



**CONTROL**

***Crb1*<sup>KO</sup>*Crb2*<sup>Low-imPRC</sup>**



ONL

INL

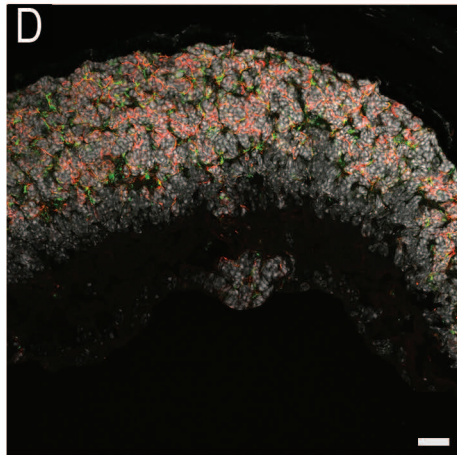
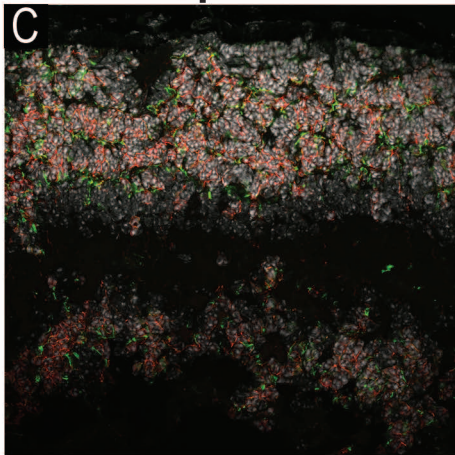
GCL

**P14**

***Crb1*<sup>KO</sup>*Crb2*<sup>ΔimPRC</sup>**

**Superior**

**Inferior**

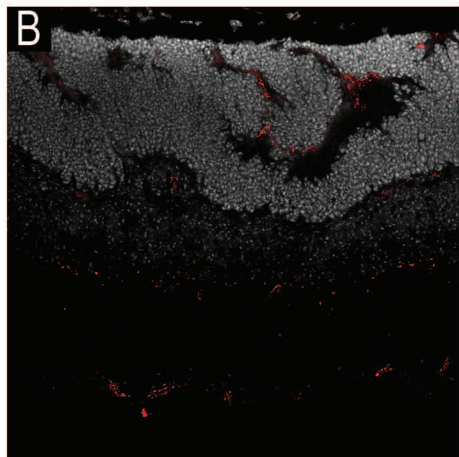
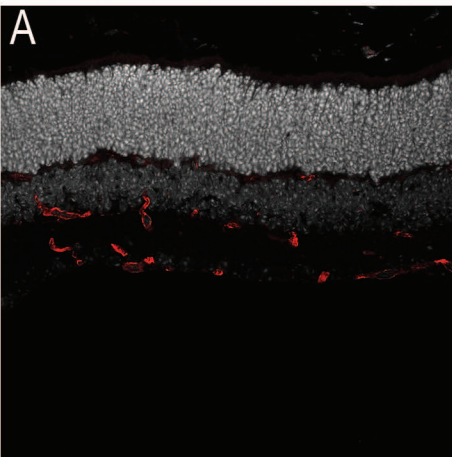


NL

GCL

**CONTROL**

***Crb1*<sup>KO</sup>*Crb2*<sup>Low-imPRC</sup>**



ONL

INL

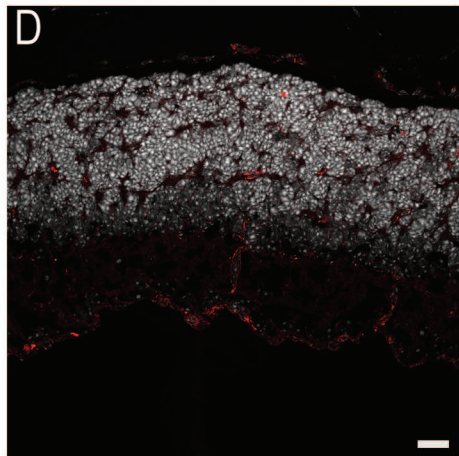
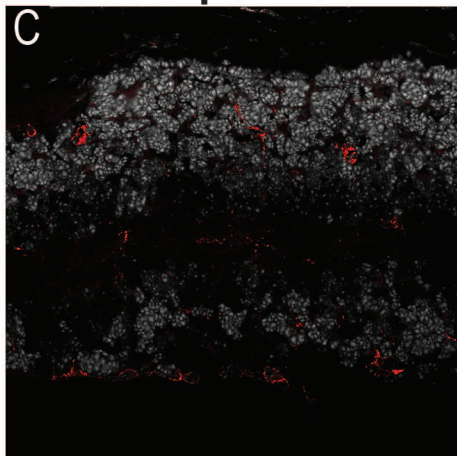
GCL

**P14**

***Crb1*<sup>KO</sup>*Crb2*<sup>ΔimPRC</sup>**

**Superior**

**Inferior**



NL

GCL